UNIVERSITY OF TURIN

DEPARTMENT OF CLINICAL AND BIOLOGICAL SCIENCES

PhD PROGRAMME IN EXPERIMENTAL MEDICINE AND THERAPY

CYCLE XXX

USE OF *Drosophila melanogaster* AS A MODEL TO STUDY CHRONIC MYELOID LEUKEMIA

THESIS' AUTHOR: SIGNORINO ELISABETTA

SUPERVISOR: PROF. CILLONI DANIELA

PhD CO-ORDINATOR: PROF. PAGLIARO PASQUALE

ACADEMIC YEARS OF ENROLMENT: 2014-2020

CODE OF SCIENTIFIC DISCIPLINE: MED/15

1. INTRODUCTION

1.1 Chronic Myeloid Leukemia

Chronic myeloid leukemia (CML) is a myeloproliferative neoplasm (MPN) characterized by the presence of a specific chromosomal aberration, the Philadelphia chromosome (Ph) (Figure 1), arising from a reciprocal translocation between the long arms of chromosomes 9 and 22, t(9;22)(q34;q11.2). This translocation results in a fusion oncogene between the *Breakpoint Cluster Region* (*BCR*) sequence on chromosome 22 and the *Abelson* tyrosine kinase (*ABL1*) gene on chromosome 9, that encodes for the constitutively active tyrosine kinase BCR-ABL1[1,2].

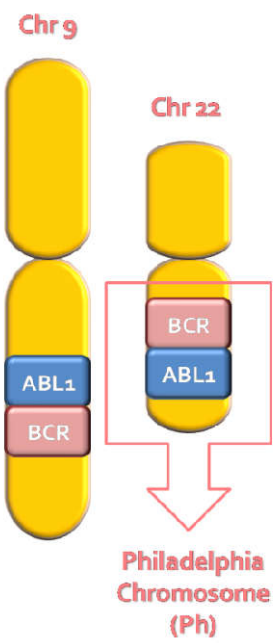

Figure 1. Schematic representation of the Philadelphia chromosome (Ph), arising from the reciprocal translocation between the long arms of chromosomes 9 and 22, that encodes for the constitutively active tyrosine kinase BCR-ABL1

CML affects the hematopoietic multipotent stem cell, and it is clinically characterized by leukocytosis with circulating mature granulocytes myeloid cells and their precursors, marked myeloid hyperplasia in the bone marrow, high platelet count and splenomegaly. It is a typically multi-phase disease, which begins with a chronic phase, mostly asymptomatic, in which the proliferation of myeloid cells is accompanied by a persistent maturation ability. After a time ranging from a few months to many years (on average 3-4 years), the chronic phase irremediably evolves into a blastic phase, assuming the characteristics of maturation block typical of acute

leukemias. There is frequent finding of an accelerated phase, of variable duration, which precedes the myeloid blast phase and is characterized by the progressive loss of the maturation ability of bone marrow cells, with an increase in blasts and promyelocytes and signs of anemia, thrombocytopenia and basophilia[3].

1.1.1. Molecular pathophysiology

In the early 1960s, the existence of a particular chromosome in bone marrow cells was demonstrated in 90-95% of subjects affected by CML, called the Philadelphia chromosome (Ph), which derives from the balanced reciprocal translocation between the long arms of the chromosomes 9 and 22[4]. In the 1980s it was possible to identify the two genes involved in translocation: the *ABL1* gene on chromosome 9 and the *BCR* gene on chromosome 22[5,6]. Following the chromosomal rearrangement the *ABL1* gene is moved from chromosome 9 to 22, where it is inserted within the *BCR* gene. The two form a new fusion gene, *BCR-ABL1*, transcribed to mRNA and translated into a new protein.

ABL1 is a nonreceptor tyrosine kinase ubiquitously expressed, while BCR is a kinase whose functions are still mostly unknown. ABL1 is usually located to the nucleus in normal cells, but the fusion with BCR moves ABL1 to the cytoplasm, enabling it to interact with several proteins and exert its leukemogenic effect. The fusion protein BCR-ABL1 becomes constitutively active, and through autophosphorylation generates several binding sites for proteins that possess an SH2 domain[7]. The leukemogenic pathway activated by BCR-ABL1 has been linked to changes in growth factor dependence, apoptosis, proliferation and cell adhesion, causing uncontrolled proliferation of granulocytes in the initial stages of the disease. The most relevant activated pathways include RAS/RAF1/MEK/ERK, PI3K/AKT, and SFKs/STAT1/STAT5[8-13], that in physiological conditions are switched on by binding of growth factors or cytokines. BCR-ABL1 presence abrogates this dependence by activating downstream proteins through direct interaction or via the GRB2/SOS/GAB2 complex. Constitutive activation of these pathways induces reactive oxygen species (ROS) formation and DNA double-strand breaks, causes uncontrolled proliferation,

DNA repair defects, dysregulates cell adhesion, and inhibits apoptosis and autophagy[14-16]. BCR-ABL1 also activates MYC, which is related to drug resistance, aberrant DNA synthesis, and genomic instability, and its levels at diagnosis may predict treatment response and progression[17]. BCR-ABL1 formation is crucial in transforming the hematopoietic stem cells and initiating CML. Further secondary cytogenetic, molecular, and epigenetic alterations provide a significant proliferative and survival advantage to committed myeloid progenitor cells and lead to blastic transformation[18,19]. The acquisition and accumulation of these alterations is due, at least partially, to the genomic instability caused by BCR-ABL1 itself[20] (Figure 3). Despite being BCR-ABL1 one of the most studied oncogenic protein, some mechanisms underlying the inexorably progression of the disease remain enigmatic. In particular, some interactors acting as positive or negative regulators of BCR-ABL1 are still unknown.

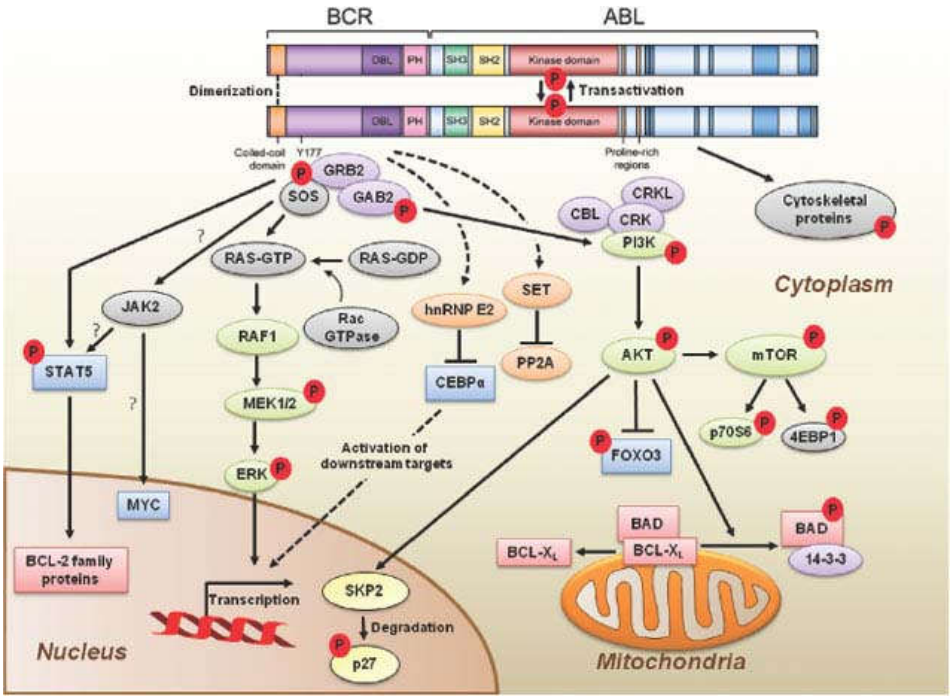

Figure 3. BCR-ABL1 most relevant activated pathways

1.1.2. BCR-ABL1 isoforms

Different breakpoints (intronic) in both *BCR* (after exon 1, 13, 14 and 19) and *ABL1* (before exon 2) genes generate the three most common fusion transcripts translated into a 190 kDa (BCR-

ABL1^{p190}), a 210 kDa (BCR-ABL1^{p210}) and a 230 kDa (BCR-ABL1^{p230}) proteins that activate multiple signaling pathways resulting in increased survival and proliferation of hematopoietic progenitors[1,21]. BCR-ABL1^{p210} is the most diffuse isoform in CML patient, whereas BCR-ABL1^{p190} is usually associated with acute lymphoblastic leukemia, but it can be found also in CML patients as an alternative splicing form of BCR-ABL1^{p210}. BCR-ABL1^{p230} is found mainly in the rare chronic neutrophilic leukemia[22] (Figure 2).

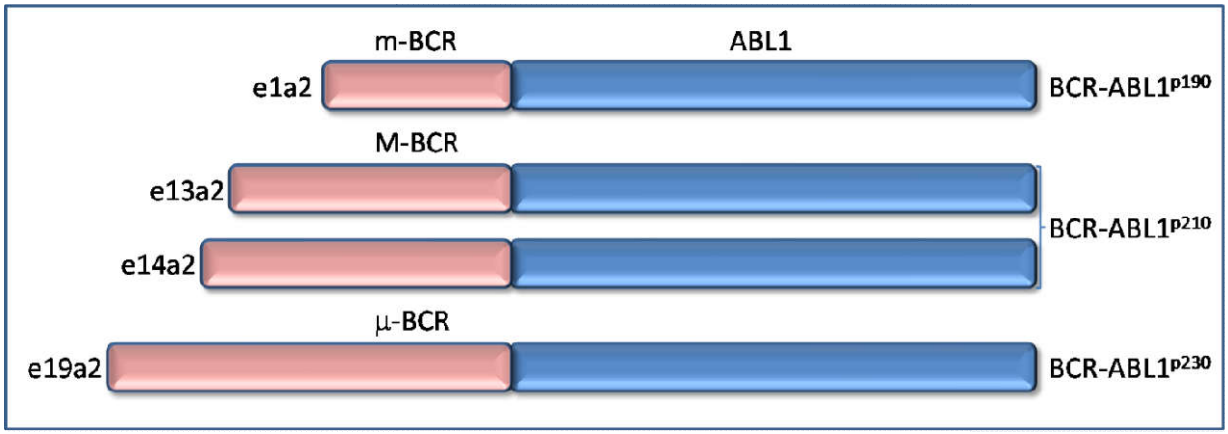

Figure 2. Most common BCR breakpoints resulting in different BCR-ABL1 isoforms

1.1.3. Epidemiology and aetiology

The incidence of CML varies from as low as 0.4/100,000/year in some non-Western countries to 1.75/100,000/year in the USA. CML is more common in males than in females with a median ratio of 1.4:1[23]. In western countries the median age of CML patients is about 57 years[24] and is responsible for 15-20 % of leukemias in adults [21]. Overall survival (OS), comorbidities, the development of complications are variables strongly influenced by age, making it an important factor in choosing the appropriate therapy[24]. Over 90% of cases are diagnosed in the chronic phase and 50% of diagnoses are occasional[21]. The aetiology of CML is essentially unknown. The only known risk factor is represented by ionizing radiation, as demonstrated by the increased incidence of this disease in the survivors of the events of Hiroshima and Nagasaki and by in vitro data[25].

1.1.4. Clinic and Diagnosis

CML evolves through a partially understood multistep process. Usually CML is diagnosed in chronic phase (CP), but without appropriate treatment the disease is bound to evolve to an accelerated phase (AP) and finally to a blast crisis (BC), where bone marrow cells lose the ability to terminally differentiate and they proliferate uncontrollably[1,22]. At onset, more than half of patients report no symptoms and the disease is diagnosed simply through a blood count, performed for various reasons, which shows leukocytosis, often with a leukocyte count higher than 100,000/mm^3, eosinophilia and basophilia. In about 30% of cases thrombocytosis occurs, very rarely anemia. A thrombocytosis with platelets greater than 450,000/mm^3 can in some cases also be the prevalent or even unique alteration of the blood count and this poses the problem of differential diagnosis with essential thrombocythemia (TE). When present, clinical symptoms are generally faded and include asthenia, night sweats, weight loss and low grade fever; other symptoms may be related to splenomegaly, that must be assessed via physical examination, present in 40-50% of cases. The marked myeloid expansion is responsible for most of the symptoms and clinical signs of the disease. The examination of the peripheral blood smear shows the entire range of precursors, from metamyelocytes to, sometimes, blasts, with the prevalence of myelocytes and promyelocytes[3,26,27]. Furthermore, morphological alterations of platelets and of red blood cells can be observed. Other altered blood chemistry tests are increased LDH levels and uricemia, typical signs of leukocytosis and increased catabolism of DNA.

The diagnosis of Ph-positive CML must be confirmed by the presence of the translocation t(9; 22) in cytogenetics, with chromosome banding analysis (CBA) or fluorescent in situ hybridization (FISH), and of the hybrid transcript BCR-ABL1, with PCR amplification techniques both qualitative (RT-PCR) and quantitative (qRT-PCR), on peripheral blood and/or bone marrow aspirate. The qualitative PCR testing is mandatory to identify the breakpoints of BCR-ABL1 present that will need follow up in therapy. In 2–4% of patients atypical BCR-ABL1 transcripts can be found, either lacking ABL1 exon2 (e13a3 or e14a3) or with different BCR breakpoints (e1a2,

e6a2, e8a2, or e19a2) that may give a false negative result with routine protocols. On the other hand, the quantitative PCR is not mandatory at diagnosis. If molecular testing highlights BCR-ABL1 presence, but the CBA is negative for the Ph chromosome, a FISH test is required[24]. About 10% of patients with a clinical picture of CML do not highlight the Ph chromosome; however, at least half of these patients have the BCR-ABL1 fusion gene, which is formed following more complex chromosomal events: in these cases we speak of masked Ph. A small group of patients negative for both chromosomal rearrangement and molecular defect is classified as true Ph-negative (Ph^-) CML, or atypical CML, which is considered a distinct form of myeloproliferative disorder, with a sometimes more severe prognosis. Bone marrow aspirate and bone marrow biopsy show the characteristic granulocytosis with expansion of the proliferating component (myeloblasts and promyelocytes) and megakaryocyte. An increase in fibrosis can be found especially in the advanced stages of the disease. As mentioned above, the progression to blast crisis represents the natural clinical evolution of the disease. Given the extreme variability of the time of progression and survival, many studies have investigated the possible presence of prognostic factors to predict the probability of dying from CML, that can guide therapeutic choices. Among these, the popular Sokal index[28], developed in the pre-interferon era and used in all TKIs trials, takes into consideration 4 factors: age, the percentage of blasts in peripheral blood, volume of the spleen and platelet count. However now, with TKI treatments most patients die during remission from causes other than CML, so the new EUTOS Long Term Survival (ELTS)[29,30] score is recommended. Based on TKI-treated patients, the ELTS score uses the same simple data as Sokal, but with negative prognostic value of age, since it has less impact in TKI-treated patients[24].

Molecular response must be evaluated as the ratio of BCR-ABL1 to ABL1 transcripts, and must be expressed as BCR-ABL1 percentage on a log scale (1%, 0.1%, 0.01%, 0.0032%, and 0.001% correspond to a decrease of 2, 3, 4, 4.5, and 5 logs, respectively). BCR-ABL1 value equal or inferior to 1% correspond to complete cytogenetic remission, (CCyR)[31]. BCR-ABL1 transcript level ≤0.1% is defined as major molecular response (MMR) or MR^3. A BCR-ABL1 transcript level

≤0.01% or undetectable disease in cDNA with >10,000 ABL1 transcripts is defined as MR^4. A BCR-ABL1 transcript level ≤0.0032% or by undetectable disease in cDNA with >32,000 ABL1 transcripts in the same volume of cDNA used to test for BCR-ABL1 is defined as $MR^{4.5}$[32].

1.1.5. Therapy

In the last 40 years, CML therapy has undergone at least three moments of great transformation, due first to the introduction of allogenic bone marrow transplant, subsequently to recombinant alpha interferon and especially, in more recent years, to imatinib, an ABL1 specific tyrosine kinase inhibitor, which is also considered the progenitor of the so-called "targeted therapy". This last drug has in fact allowed to radically change the prognosis of patients with CML and even to bring the life expectancy of these patients similar to those of the control population of the same age[24,33].

As soon as it was introduced into clinical practice in the late 1970s, allogeneic bone marrow transplantation (now allogenic stem cells transplantation, allo-SCT) became a fundamental therapeutic aid for patients with a compatible HLA donor and at an age in which the toxicity of the procedure was still sufficiently tolerated. Transplantation is in fact still considered the only therapy potentially capable of eradicating the Ph-positive (Ph^+) leukemic clone and definitively healing the disease. This result of bone marrow transplantation is not achieved so much with initial chemo-radio conditioning therapy, but through an immune-mediated mechanism of graft versus leukemia (GVL), which probably represents an aspect (in this case therapeutically useful) of graft versus host disease (GVHD). However, the introduction of TKIs in CML therapy has in fact greatly limited the use of bone marrow transplantation, reserving it only for the few patients resistant to multiple inhibitors or in an advanced stage of disease.

Conventional chemotherapy was used for the purpose of controlling clinical symptoms and leukocytosis, but was unable to induce cytogenetic remission and significantly influence the patient's prognosis. Hydroxyurea (HU) is still the drug of choice when opting for chemotherapy alone, or to control symptoms while waiting for testing results.

Recombinant alpha interferon (r-IFNα) was the first drug to be effective in inducing cytogenetic remission of CML, thus in the pre-TKIs era was the treatment of choice. The association of the r-IFNα with Cytarabin (ARA-C) cycles allowed to obtain a higher percentage of cytogenetic remissions even if with a certain increase in toxicity (nausea, asthenia, pancytopenia)[34]. Now a pegylated (PEG) form is available, and several trials of PEG-IFNα in combination with different TKIs are ongoing to help increase the patients that could qualify for drug discontinuation, the new goal in CML treatment.

Nowadays, first line treatment for all CML patients but pregnant women is a first (imatinib) o second (dasatinib, nilotinib, bosutinib and radotinib, le latter approved in South Korea only) generation TKI (2GTKI).

Imatinib mesylate (formerly STI571 and commercially called Glivec, Novartis), is a selective inhibitor of ABL1, BCR-ABL1 and tyrosine kinase activity mediated by a few other cellular protein tyrosine kinases (PDGFRα and β, c-KIT) thus resulting as an active growth inhibitor of Ph^+ cells and without significant effects on normal bone marrow and other tissues[35]. It binds ABL1 ATP-binding site, thus preventing the phosphorylation of ABL1, and BCR-ABL1, substrates (Figure 4).

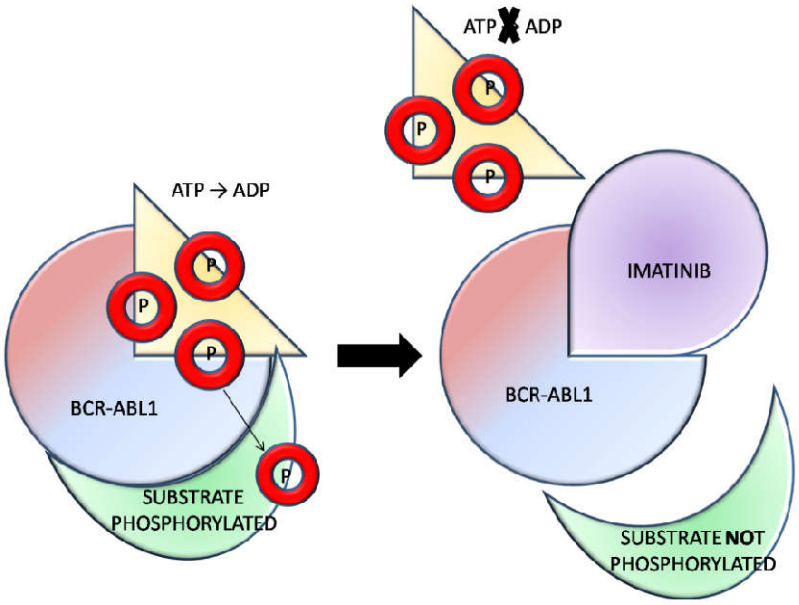

Figure 4. Mechanism of action of specific BCR-ABL1 inhibitor imatinib.

Imatinib, at a dosage of 400 mg/day per os, currently represents treatment of choice for newly diagnosed patients in the chronic phase of the disease. A lower dose of 300 mg can be used if 400 mg is not tolerated. The dose can be raised to 400 mg twice daily in AP, however in more advanced disease switching to a 2GTKI is recommended. This drug is able to determine the achievement of a complete cytogenetic remission in over 80% of treated patients[36]. At 5 years, MMR rates range between 60–80% and OS range between 90–95%[24]. Generic imatinib is now available worldwide.

Resistance to imatinib is observed in about 15-20% of patients treated early in the chronic phase, but is higher in the advanced stages of the disease. It can be of two types: primary (absence of ab initio response) or secondary (appearance of resistance during therapy). The molecular mechanisms underlying imatinib resistance can be traced back to two main categories: (a) those in which BCR-ABL1 maintains residual tyrosine-kinase activity, among whose causes are point mutations, receptor gene amplification and insufficient cellular imatinib concentration; (b) those in which BCR-ABL1 is completely inhibited by imatinib, but clonal proliferation is supported by the activation of other molecular pathways or additional chromosomal aberrations (ACAs). Point mutations are certainly among the best known and most studied mechanisms and they can affect several functional domains of BCR-ABL1[37]. It should be noted that not all mutations confer absolute resistance to the drug: the increase in the inhibitor dosage can often overcome them, thus obtaining a satisfactory response[38]. In other cases, 2GTKI, such as dasatinib, nilotinib and bosutinib are able to overcome imatinib resistance in second-line treatments[37]. Switching to a second line treatment can also be due to patients related intolerance.

Dasatinib is active in presence of several BCR-ABL1 mutations[39]. It is more potent than imatinib, giving a faster an deeper MMR, but OS is similar to imatinib. The approved dose for CP patients is 100 mg/day, while for advanced phases is 70 mg twice daily. Another 2GTKI more potent than imatinib and active in presence of BCR-ABL1 mutations is nilotinib. The approved dose is 300 mg twice daily in case of first-line treatment and it is raised to 400 mg twice daily if treatment is started

in second-line. Bosutinib is the third 2GTKI and is also more potent than imatinib and exhibit activity against several BCR-ABL1 mutants. The approved dose is 400 mg/day when used in first-line, and raised to 500 mg/day in second-line. Radotinib, a fourth 2GTKI, has been approved in South Korea, and it is structurally similar to nilotinib and shows an almost identical activity against BCR-ABL1 mutants[24].

All 2GTKIs and imatinib are ineffective against BCR-ABL1^{T315I} mutation, as this mutation occurs in the ATP binding site of ABL1, where these drugs also bind. Ponatinib, a third generation TKI more potent than all others, is the only one approved for treatment of patients bearing BCR-ABL1^{T315I} mutation, as for patients resistant to two or more TKIs. The approved dose is 45mg/day, but given the cardiovascular toxicity, dose can be lowered to 30 or 15mg/day[24]. Asciminib is the first allosteric ABL1 kinase inhibitor to reach clinical evaluation phase. It was designed to target the BCR-ABL1^{T315I} mutation while possibly avoiding the cardiovascular toxicity of ponatinib. Unlike all the others TKIs, that bind the ATP binding site, asciminib binds to the myristoylation pocket of BCR-ABL1, which is responsible for regulation of ABL1 kinase activity. Clinical evaluation is still ongoing, but preliminary data suggest that resistance mutations problematic for asciminib reside exclusively in and around the myristoylation pocket[37].

imatinib			dasatinib	nilotinib	bosutinib	ponatinib	asciminib
M237 V	F311L	V379I	V299L	L248R	L248R	T315M/L	**A337**
M244V	**T315I**	A380T	**T315I**	Y253F/H	G250E/R		**W464**
L248R	F317L/V/I/C	F382L	F317L/V/I/C	E255K/V	E255K/V		**P465**
G250E/R	F359V/I/C	L384M		**T315I**	**V299L**		**V468**
Q252R/H	Y342H	L387M/F		F317L/V/I/C	**T315I**		**I502**
Y253F/H	M343T	M388L		F359V/I/C L	F317L/V/I/C		
E255K/V	A344V	Y393C					
E258D	M351T	H396R/P					
V L273M	E355D/G	A397P					
E275K/Q	F359V/I/C	S417F/Y					
D276G	D363Y	I418S/V					
T277A	L364I	S438C					
E279K	A365V	E453G/K					
V280A/I	L370P	E459K/V					
V289A	V371A	P480L					
V299L	E373K	F486S					

Table 1. List of the most frequent BCR-ABL1 point mutations that confer resistance to TKIs. Residues at which mutations are associated with strong resistance to a given TKI are indicated in bold underlined.

BCR-ABL1 mutations (Table 1) are still usually detected by Sanger sequencing (approximately 20% sensitivity), but currently NGS is recommended whenever possible given the higher sensitivity

of about 3%, raising the possibility of early relevant BCR-ABL1 mutations in patients resistant to TKIs treatments[40,41].

When patients fail to respond to two or more TKIs, allo-SCT is still the therapy of choice, especially if it is resistant to 3 months ponatinib treatment as well[24].

When CML is diagnosed in AP, the patient is considered high-risk and eligible for allo-SCT if response to therapy fails. Instead a patient progressing to AP or BC should be immediately tested to find a donor for allo-SCT. For patients diagnosed in or progressing to BC, the disease should be controlled with chemotherapy (with regimes for AML or ALL) plus a TKI before transplantation[24].

1.2. Drosophila melanogaster

1.2.1. Model organism

A promising new approach for the identification of candidate genes and for the study of the molecular pathways involved in disease onset and progression is represented by the use of the fruit fly *Drosophila melanogaster*.

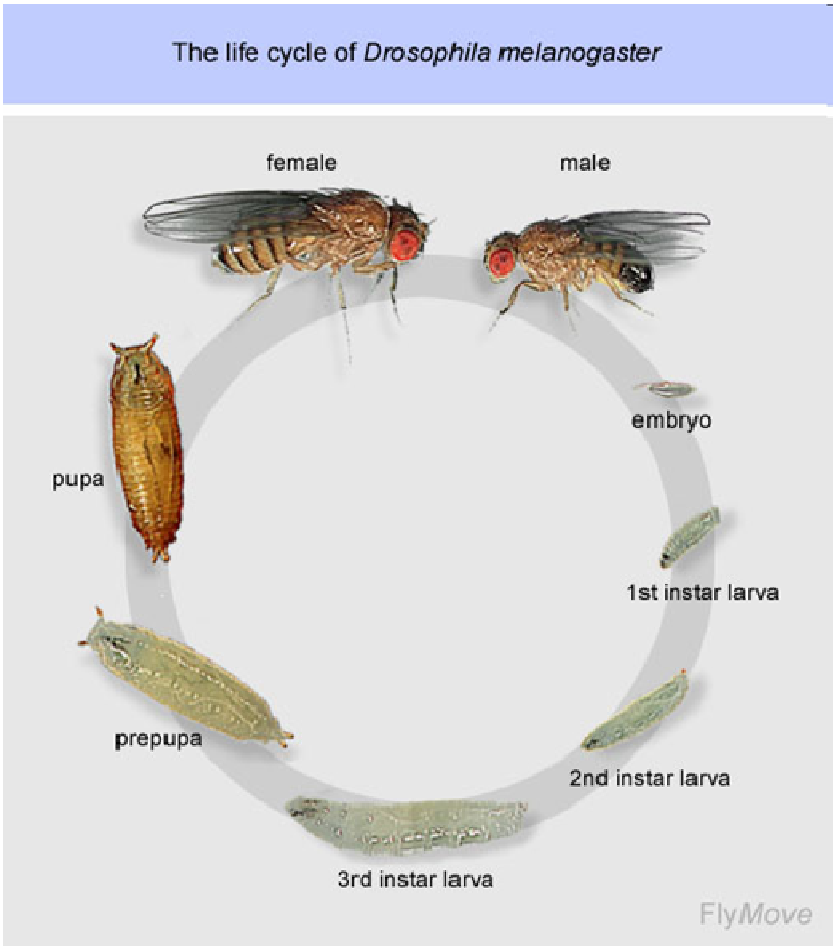

Figure 5. *Drosophila melanogaster* life cycle

Drosophila has been one of the most used model organisms for genetic studies for over a century. The first studies date back to 1910 when Thomas Hunt Morgan used the fruit fly to carry out his studies on inheritance linked to the X chromosome. The cost-effectiveness and speed (given by the very short life cycle, Figure 5) of the studies, the high number of offspring that is obtained in one generation, the development of numerous genetic tools such as phenotypic markers and balancing chromosomes that allow recognizing the genotype by looking at the phenotype of the fly and the

absence of recombination in the male are in fact undoubted advantages related to the use of this "tool" in biological research. In addition, the completion of the sequencing of the *Drosophila* genome, consisting of only 4 pairs of chromosomes (3 autosomes, chromosomes 2, 3 and 4 and one sexual, X/Y) and more than 13000 genes, highlighted a high homology between the human and *Drosophila* genome, extended also to genes involved in the pathogenesis of various diseases[42] (over 60% of the human genes known to be involved in human pathologies have in fact an ortholog in *Drosophila*); this high homology combined with low gene redundancy makes *Drosophila* a very useful genetic model for the study of various human diseases. This model also allows the identification of new molecular pathways and the study of the role they play in the development of pathology, without requiring prior knowledge of the function of any genes involved. Finally, the identification of functional homologies between vertebrate proto-oncogenes and their ortholog in *Drosophila* [43,44] make *Drosophila melanogaster* a good candidate as a model for genetic studies also in the field of oncohaematological diseases.

1.2.2. The Gal4/UAS system to direct gene activation

The *Gal4/Upstream Activating Sequence (UAS)* [45,46]system is one of the most powerful tools for targeted gene expression. It is based on the properties of the yeast GAL4 transcription factor which activates transcription of its target genes by binding as a dimer to UAS cis-regulatory sites, a distinct 17 bp sequence. Gene expression is directed by inserting the UAS sequences, to which Gal4 binds, upstream of the transgene sequence of interest. The insertion of Gal4 in random positions in the *Drosophila* genome, has allowed to generate numerous "enhancer trap" lines that express Gal4 under the control of endogenous promoters capable of regulating the expression of transgenes in a specific time or tissue manner, for example by inducing the production of exogenous protein only at the level of the eye, wing, lymphatic gland or other tissues of the adult and larva. The expression of the transgene of interest in a specific tissue way is therefore obtained by crossing the suitable Gal4 enhancer trap line, with a transgenic *Drosophila* in which the gene of interest has been placed downstream of one or more UAS sequences[47] (Figure 6).

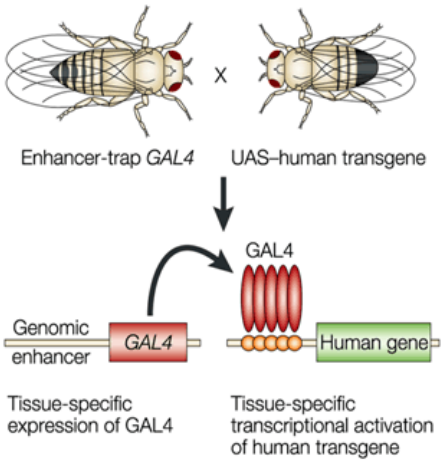

Figure 6. The yeast *Gal4/UAS* (*Upstream Activating Sequence*) transcriptional regulation system controlled by a gene promoter active in specific tissues and stages (*Gal4* drivers)

1.2.3. Generation of transgenic Drosophila

In order to generate transgenic *Drosophilae* for genes of interest, their coding sequence has to be cloned into a *Drosophila* plasmid vector downstream a 5x (pUAST) or even 10xUAS sequence (pKs69). The plasmids obtained are then microinjected into the embryos and the gene together with the UAS sequences is integrated into the genome at random sites taking advantage of particular regions similar to the transposons, called p-elements. To avoid homologous recombination (that occurs only in females) which could lead to the loss of the transgene, the transgenic lines need to be balanced: on the other allele of the chromosome where the gene is integrated, a repeated inverted sequence, lethal in homozigosity, together with a phenotypical marker, is inserted. This way the presence of the transgene can be tracked in future crossings. The most common balancer for chromosome X is the FM7, that causes the formation of heart-shaped eyes. For chromosome 2 is the CyO, that leads to the formation of curly wings. For chromosome 3 is the TM3, that creates short and thick dorsal hairs.

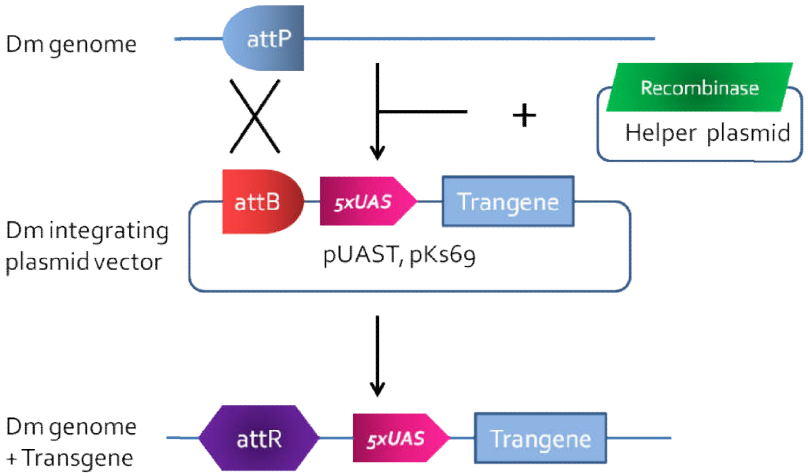

Figure 7. Generation of transgenic *Drosophila melanogaster* using p-element plasmid vectors

1.2.4. Genetic screening for dominant modifiers: enhancers and suppressors

The *Drosophila* model is often used to perform genetic screenings as it allows to identify unknown genes possibly involved in the development of a specific biological process or pathway [48,49]. One of the methods by which it is possible to identify components of a pathway of interest is the use of genetic screening for dominant modifiers, such as enhancers or suppressors. This system is based on the fact that the loss-of-function mutations are usually recessive, indicating that the remaining 50% of the wild-type protein is able to correctly maintain and perform the gene function to which it is assigned, thus ensuring normal development of that particular process. However, when a given process is already partially altered due to the presence of a mutation or overexpression of a gene thus generating a sensitive genetic background, 50% of gene function may not be sufficient to maintain the normal development of the biological process, and mutations of genes involved in that pathway can be used to identify dominant enhancers or suppressors in that genetic background. This type of approach has been used for the study and identification of components of many signal transduction pathways including those downstream of the sevenless tyrosine kinase receptor (sev), an important regulator of the R7 photoreceptor in the eye of *Drosophila* [50]. This type of screening for deletions, which are equivalent to a null mutation of all the genes that map in the region,

represents a relatively rapid method to screen the entire genome, in order to identify new genes involved in a given pathway.

1.2.5. The eye of Drosophila

The eye of *Drosophila* represents a very complex structure whose development is strictly regulated by numerous processes of both cell proliferation and differentiation involving a very large number of genes[51]. It develops from the repetition of a regular structure consisting of 700-800 ommatidia or visual units. Each ommatidium has a very precise structure that derives from 19 precursor cells and consists of 8 photoreceptors (R1-R8) and 12 accessory cells, pigmented cells and a cornea each of which is strictly regulated by type and position[52] (Figure 8). Photoreceptors secrete many varieties of rhodopsin forms and visual transduction occurs through the activation of coupled G proteins: when rhodopsin (Rh) absorbs a photon, its carotenoid chromophore isomerize, producing a conformational change in Rh in its active form, metarhodopsin [53].

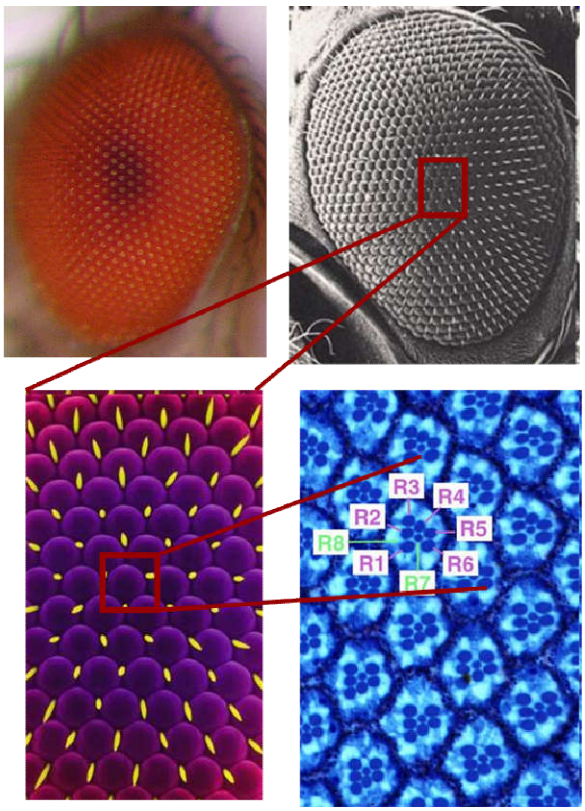

Figure 8. Schematic representation of the eye of *Drosophila melanogaster*

The eye develops during the third larval stage (3rd instar, L3) starting from a single-layer epithelium, the imaginal disc of the eye, in which the morphogenetic furrow (MF) proceeds from the posterior to the anterior portion by adjusting the assembly of the ommatidia. The eye represents one of the most used read-out systems in genetic screening as it represents an experimentally easy and accessible tissue, suitable for the analysis of gene function. Finally, it constitutes a non-vital organ of *Drosophila* which allows the expression of large amounts of exogenous proteins without resulting in lethality[51].

2. AIMS OF THE STUDY

Although the role of BCR-ABL1 in the pathogenesis of CML has been widely clarified, some of the genes and mechanisms responsible for the progression of the disease in blast crisis are still unknown. The fruit fly, *Drosophila melanogaster*, represents a powerful tool for genome-wide genetic analysis and screens, given the functional conservation and sequence homology between human and *Drosophila* genes. This approach may allow identifying genetic pathways that contribute to the disease onset and/or progression without an *a priori* knowledge of the gene function [54]. Nevertheless, the high degree of conservation between human and *Drosophila* Abl (dAbl) proteins and the existence of *Drosophila* homologs for many proteins that functionally interact with BCR-ABL1 in mammals, strongly supports the idea that dAbl and presumably BCR-ABL1 signal transduction pathways could be highly conserved from fly to human. Interestingly, Fogerty and colleagues demonstrated that the neural expression of a chimeric BCR-ABL protein carrying the human BCR fused to the *Drosophila* Abl (dAbl), is able to rescue *dAbl* mutant phenotype, suggesting that the chimeric BCR-ABL protein can effectively compensate for lack of dAbl[55].

The aims of this study were therefore:

a) the generation and validation of a genetic model based on transgenic flies that drive inducible human BCR-ABL1 expression under the control of tissue and stage specific promoters (published) [56]
b) to conduct a genome-wide genetic screening using our BCR-ABL1 transgenic Dm as 'bait' to identify novel functional interactors
c) a preliminary analysis of a candidate gene identified by the screening in patients with CML.

3. MATHERIALS AND METHODS

3.1 Generation of BCR-ABL1 *transgenic flies*

BCR-ABL1 coding sequence was PCR amplified using AmpliTaq Gold DNA Polymerase (Applied Biosystems, Thermo Fisher Scientific, Waltham, MA, USA); PCR products were isolated from agarose gel, purified using a Spin Column Kit (Qiagen, Venlo, Netherlands) and restricted with *EcoRI* and *XbaI*. The restriction fragments were cloned into the P-element expression vector, PKS69, downstream of a promoter comprised of ten tandem GAL4 binding sites referred to as UAS (Upstream Activation Sequence). The recombinant plasmid was transfected into *Escherichia coli* DH5-α strain and grew in LB (Luria Bertani) medium supplemented with ampicillin 100 μg/ml, for 18 hours at 30°C. Plasmid DNA was prepared using the Qiafilter^{TM} Plasmid Maxi Kit (Qiagen) according to the manufacturer's instructions and transformed into flies by injection in *Drosophila* embryos. (The Best Gene, Inc, Chino Hills, CA, USA); 7 independent transgenic lines have been generated. The human *BCR-ABL1 Kinase Dead* (*BCR-ABL1*^{KD}) cDNA was obtained through site-directed mutagenesis. The following mutagenic primers containing the desired mutation (Val-Met-Thr instead of Val-Lys-Thr) in the P-loop of the BCR-ABL1 tyrosine kinase domain were used: fwd GTGGCC**GTGATGACC**TTGAAGGAGG and rev TCCTTCAA**GGTCATCAC**GGCCACCG. 25ng of plasmid DNA containing the *BCR-ABL1* cDNA was PCR amplified using the Expand Long Template PCR System (Roche Applied Science, Penzberg, Upper Bavaria, Germany) according to the manufacturer's instructions. The non-mutated parental methylated DNA template was digested for 2 hours with *DpnI* and the plasmid carrying the desired mutation was finally prepared using the Qiafilter^{TM} Plasmid Maxi Kit (Qiagen, Venlo, Netherlands). Plasmid DNA was injected into *Drosophila* embryos (Trans-FlyER, Startup Company, Ferrara, Italy) and 3 independent transgenic lines were obtained.

3.2 Drosophila stocks

The following fly stocks, enhancer trap lines, deficiencies and mutants were obtained from the Bloomington Stock Center (Department of Biology, Indiana University, Bloomington, IN, USA)

and they are described at FlyBase (flybase.bio.indiana.edu): Oregon R (adopted as wild type strain), *gmrGal4* (P(Gal4-*gmr*)-3rdchr.)[52], *sevenlessGal4[57]*, *STAT92E^{06346}* (stock# 11681) *UAS-Abl* (#8567), *UAS-Abl^{K417N}* (#8566), *Abl[1]* (#8566), *Df (3L)st-f13 (fax deficiency-Df*, #2993), *Df(3R)T-32 (pros Df,* #3003), *Df(3L)81k19 (dab Df, #2998), Df(2R)P34 (ena Df, #757), fax[M7]* (#8786), *pros[17]* (#5458), *Dab EY10190* (#16974), *ena[23]* (#8571), Deficiency kits for chromosome 2 (DK2L and DK2R) and 3 (DK3L and DK3R), Rab5.S43N (#9771), UAS Rab5 wild type (#24616), UAS Rab5.Q88L (#9773). RNA interference (RNAi) lines for *Abl* (#2897), *Dab* (#14008 and #13005) and *ena* (#43056 and #106484) were obtained from VDRC (Vienna *Drosophila* RNAi Center, Wien, Austria). *domelessGal4* (from Noselli S.[58]) and *STAT^{DN}* (from Betz A.[59]) fly stocks were kindly provided by A. Giangrande (IGBMC, Illkirch, France). In order to generate a sensitive genetic background in flies and to express transgenes in a tissue specific pattern, flies carrying the *BCR-ABL1* transgene were crossed with flies expressing the yeast transcriptional activator Gal4 in the eye imaginal disc (*sevGal4* and *gmrGal4*). Flies were cultured in standard medium and grown at 25°C, if not otherwise specified. To study the eye phenotypes, images of adult eyes were captured using a stereomicroscope equipped with a photo-camera (Olympus, Olympus Italia srl, Segrate MI, Italy, or SMZ1500, Nikon Instruments, Amsterdam, Netherlands). Oregon R wild type strain was used as control if not otherwise specified.

3.3 Immunoblotting and immunoprecipitation

Adult heads (0-5 days old) were dissected and homogenized in a protein extraction buffer (**fly heads:** Tris-HCl pH 7.4 10mM, NaCl 150mM, EDTA 5mM, EGTA 5mM, Glycerol 10%, DTT 5mM, Urea 4M, supplemented with protease (CLAP cocktail containing Chymostatin 25mg/ml, Leupeptin 25mg/ml, Antipain 25mg/ml and Pepstatin A 25mg/ml, use 1:1000) and phosphatase (Sodium Orthovanadate 1mM) inhibitors; **cell lines:** Tris-HCl pH 8 50mM, NaCl 150mM, Np40 1%, DOC 0,5%, SDS 0,5% supplemented with protease and phosphatase inhibitors). Lysates were incubated on ice for 30 minutes followed by centrifugation at 18000 g for 15 minutes at 4°C.

Proteins (50 μg) were denatured in 4X SDS Laemli's buffer by boiling for 5 min, resolved on a SDS 8% polyacrylamide gel and transferred to a nitrocellulose membrane (Amersham Bioscience, GE Healthcare, Waukesha, WI). The membrane was blocked for 1 h at room temperature with 5% BSA (Bovine Serum Albumin; Sigma-Aldrich Corp., St. Louis, MO) in 1X Tris-buffered saline (TBS) and then probed overnight at 4°C with primary antibodies in 1% BSA 1X TBS-tween buffer. Detection was performed using anti-mouse IgG HRP-conjugated secondary antibodies (anti-mouse sc-2005, anti-rabbit sc-2004, Santa Cruz Biotechnology, Santa Cruz, CA, USA) for 1 h at 4°C. For Immunoprecipitation, 1 mg of total protein extract was incubated for 3h at 4°C with 4 μg of anti-Enabled supernatant and subsequently for 45 min at 4°C with Protein A Sepharose (Amersham Bioscience, GE Healthcare, Waukesha, WI, USA). Proteins signal intensities were measured using a Java software (Image J). Unless noted differently, each experiment was repeated three times on biologically independent samples. The following primary antibodies were used: c-Abl (sc-23), Dab1 (sc-271136), p-Tyr (sc-7020), GAPDH (sc-137179)(Santa Cruz Biotechnology, Santa Cruz, CA), α-Tubulin (CP06; Oncogene Research Products, Merck KGaA, Darmstadt, Germany) mouse monoclonal antibodies, BCR (sc-20707) rabbit polyclonal antibody (Santa Cruz) and mouse 5G2 anti-Enabled supernatant (Developmental Studies Hybridoma Bank-DSHB, University of Iowa, IA). For Immunoprecipitation, 1 mg of total protein extract was incubated with anti-Enabled supernatant and subsequently with Protein A Sepharose (Amersham Bioscience, GE Healthcare, Waukesha, WI).

3.4 Fluorescent Immunolabeling

Fly eye primordium. Eye imaginal discs were dissected from third instar larvae, fixed in 4% paraformaldehyde in 1X PBS for 20 minutes, permeabilized with 0,3% Triton X-100 for 1 hour, labeled with the rat anti-Elav 7E8A10 supernatant (DSHB) diluted 1:50 in 1X PBT (0.1% Triton X-100 in 1X PBS) overnight at 4°C, incubated with a Cy3-conjugated anti-rat secondary antibody (Jackson Immunoresearch, Newmarket, UK) for 2 hours and exposed to HOECHST (Sigma-

Aldrich Corp., St. Louis, MO) before mounting in Fluormount-G (Electron Microscopy Sciences, Hatfield, PA).

Primary cells. Protocol was approved by the local ethic committee (number of approval 212/2015). 10^5 white blood cells were obtained from peripheral blood, cytospinned for 5 minutes at 300 rpm, fixed with 4% PFA and permeabilized with 0.1% Triton X-100 for 3 min. Cells were blocked with PBS containing 10% BSA for 45 min. Cells were then stained with primary antibodies overnight at 4°C. The antibody–antigen complexes were detected by incubation for 1 hour with secondary antibody. Cells were treated with DAPI (Sigma-Aldrich Corp., St. Louis, MO, USA) for 5 min to stain the nucleus. Primary antibodies mouse anti-Dab1 and anti-Dab2 (sc-271136 and sc-136963, Santa Cruz) and anti-mouse Alexa Fluor 568 secondary antibody (Molecular Probes-Invitrogen, ThermoFisher Scientific, Waltham, MA) were used.

Immunolabeled imaginal discs or cells from patients were analyzed, respectively, with Nikon A1R confocal laser-scanning microscope, equipped with a Nikon PlanApo 40x lens and captured using NIS Elements AR 3.10 software (Nikon) or with fluorescence microscope (DM2000 LED, Leica Microsystems, Wetzlar, Germany) and captured using 100x oil immersion objective. Fluorescent signal from cells was measured by Image Processing and analyzed with Graphpad Prism 7.

3.5 Genetic analysis

Eye. Flies carrying *gmrGal4* or *sevGal4* driver constructs have been crossed to the *UAS-BCR-ABL1* transgenic lines. To analyze the phenotype, flies from a recombinant line carrying both *gmrGal4* and *UAS-BCR-ABL1* on the 3rd chromosome (*gmrGal4,UAS-BCR-ABL1 4M/TM3*) were crossed to lines carrying single gene mutations, deficiencies, RNAi constructs or chromosomal deletions. 15-30 F1 flies from three independent crosses were classified in three or five phenotypic classes described in the Results section.

Melanotic nodules. *domelessGal4* driven BCR-ABL1 expression was controlled with the TARGET system[60,61]. The constitutive expression of the oncoprotein BCR-ABL1 under the control of the *domelessGal4 (domeGal4)* induces a fully penetrant lethality. This early lethality phase is due to

domeGal4 activity in essential tissues other than the lymph gland. To overcome this problem and analyze the effect of BCR-ABL1 overexpression in the hematopoietic precursor cells of the lymph gland Medullary Zone, we ubiquitously expressed under the control of the *tubulin* gene promoter a temperature-sensitive mutant of Gal80 (*tubulin-Gal80^{TS}*) that represses Gal4 activity by binding to the Gal4 transcriptional activation domain. Gal80^{TS} is active at 18°C and inactive at 29°, releasing the Gal4 activity from repression (temporal and regional gene expression targeting - TARGET system[60-62]). *domelessGal4; UAS-BCR-ABL1 3M; tubulin-Gal80^{TS}* synchronized larvae were kept at 18°C until the indicated instar then they were exposed to 29°C to inactivate the Gal80^{TS} protein and release Gal4 transactivation activity. Analysis of the melanotic nodule phenotype and temperature shift experiments have been performed as previously described[63].

3.6 RNA extraction and quantitative analysis

RNA was extracted using TRI Reagent Solution (Ambion, Thermo Fisher Scientific, Waltham, MA, USA), following the manufacturer's instructions and 1µg was used as a template for the reverse transcription reaction in a finale volume of 25µl.. Expression levels of *Dab1*, *Dab2* and *RAB5A* were evaluated by RealTime PCR with TaqMan Universal Master Mix (Applied Biosystems) using CFX96 Real-Time PCR Detection System (Bio-Rad Laboratories) by using 5 µL of cDNA (1/10 of retrotranscription product) and using specific assays on demand kits of primers and probe following the manufacturer's instructions (Hs00245445_m1 for *ABL1*, Hs00221518_m1 for *Dab1*, Hs00184598_m1 for *Dab2,* Hs00939627_m1 for *GUSB*, Hs00991290_m1 for *RAB5A*, Applied Biosystems, ThermoFisher Scientific). The analysis was performed in duplicate and results showing a discrepancy of >1 Ct in one of the wells were excluded and repeated. qRT-PCR data were analyzed by CFX Manager Software (Bio-Rad Laboratories). Universal Human Reference RNA (#740000-41, Stratagene, La Jolla, CA, USA) was used as calibrator.

3.7 Patients and cell line

For *Dab1* and *Dab2* expression study for, 103 bone marrow aspirate (BM) and peripheral blood (PB) samples from 95 CML patients and 20 healthy donors were collected from the San Luigi Hospital. Eight patients were analyzed during follow up. Buffycoat was performed to obtain white blood cells. K562 cell line (ATCC, Manassas, VA) was used for transfection and proliferation assays. K562 cell line was maintained in RPMI 1640 and supplemented with 10% of foetal bovine serum (FBS). Cells were grown at 37°C in a humidified atmosphere flushed with 5% CO_2.

For *RAB5A* expression study, 87 BM and PB samples from 56 CML patients and 16 healthy donors were collected from the San Luigi Hospital. Informed consent was obtained from each patient and the San Luigi Hospital Institutional Review Board approved the study (212/2015). All samples were de-identified and cases anonymized by diagnostic staff members not involved in the study. Clinical parameters were compared and analyzed through coded data: 31 samples were collected at diagnosis, 23 at least in cytogenetic remission and 7 during secondary resistance. In addition, other 10 specimens were collected from patients during primary resistance to TKI. Buffycoat was performed to obtain white blood cells.

3.8 K562 transfection

30 µg of pReceiver-M07-Dab1 Vector containing the whole *Dab1* coding sequence (GeneCopoeia™, Rockville, MD, USA) was electroporated in K562 cell line using the GenePulser™ electroporation apparatus (Bio-Rad Laboratories) under the following conditions: 1 pulse at 300Volt and 75mF capacitance. Electroporation with 30 µg pEGFP alone was performed as control.

3.9 Proliferation assay

Transfected cells were seeded at $10x10^4$ concentration in RPMI with 10% FBS for 18 hours and then starved. After 12 hours, 10% FBS was added and finally 6 hours later 1 µCi/ml ^{3}H-Thymidine was added (GE Healthcare). After 24 hours of incubation, the ^{3}H-Thymidine was removed; cells were then washed with PBS and 5% trichloric acetic acid and resuspended with NaOH. The amount

of incorporated ^{3}H-Thymidine was detected using a β-counter. Experiments were performed in triplicate.

3.10 Statistical analysis for validation of the model

The statistical significance of difference between distributions of the adult eye phenotypic classes considered in the different experimental sets has been evaluated applying the Mann-Whitney test. The difference of the melanotic nodules phenotype between the compared different genotypes were validated by applying the two-tailed Student's t-test to data from at least three independent experiments and calculating the p-value using the software GraphPad Prism 5. The expression data of Dab1 and Dab2, and the Dab1 proliferation data, were analyzed with the Student's t-test, the p-value calculated using the software GraphPad Prism 7.

3.11 Bleeding, preparation of hemolymph samples and estimate of the circulating hemocytes.

Three groups of ten late L3 instar larvae conditionally expressing BCRABL1 under the control of the *domeGal4* driver or larvae carrying only the *domeGal4* construct as negative control, were bled into 30 µl of PBS1X, labeled for 20 min at room temperature with Cy3 conjugated Phalloidin (20µg/ml, Sigma) that binds filamentous actin. The nuclei were labeled 5 min at room temperature with HOECHST 33342 (10µM Sigma) that is able to enter into unfixed alive cells. The bled circulating hemocytes were mounted on a slide under a 20x20 mm coverslip adding 5µl of Fluormount. In order to estimate the number of circulating hemocytes, cells co-labeled by Phalloidin/HOECST were counted in three random fields of three slides representing biological replicas. The average number of hemocytes per field between the slides was calculated. The data were analyzed with the Student's t-test and the p-value calculated using the software GraphPad Prism 7.

3.12 Bioinformatics and statistical analysis of genetic screening data

All genes completely or partially disrupted/deleted included in each *Drosophila* stock (FBgn #) were reannotated by homemade Perl script using updated information from Bloomington *Drosophila* Stock Center (https://bdsc.indiana.edu/) and FlyBase (https://flybase.org/). Each stock was annotated in the appropriate phenotypic class (-2, -1, 0, +1, and +2). For each stock, all genes present in class 0, that did not affect phenotype if destroyed, and genes included in contrasting phenotypic classes were removed by the list of affected genes. Subsequently, the remaining genes were annotated by gene ontology and sorted in supplementary table 1 for the frequency of biological process in ameliorative (+1 and +2 class) or pejorative phenotype (-1 and -2 class).

RAB5A mRNA Cycle Threshold values (CtT) were calculated by Bio-Rad CFX manager 3.1 software and normalized against the internal control *GUSB* (CtR) by subtraction (CtT-CtR). ΔCt values generated were following standardized with ΔCt obtained by Universal reference RNA (Stratagene), evaluated in the same run. Differential *RAB5A* transcript expression between -ΔCt values of healthy controls and samples derived from each different clinical subgroup or between groups were evaluated using the t-test.

RAB5A mRNA expression levels have been dichotomized into two groups of “high” and “low” expression using median value as threshold cut-off. *BCR-ABL1* transcript presence, evaluate as percentage of *BCR-ABL1/ABL1* x 100, was dichotomized into groups using two diagnostic criteria: molecular remission (< 0.1%) and cytological remission (< 1%). The association between *RAB5A*-ΔCt and *BCR-ABL1* transcript was evaluated using the Fisher exact test. Statistical analysis was performed using R statistical software.

4. RESULTS

4.1 Expression of human BCR-ABL1 affects eye cell differentiation

The first aim of this work was to set up a CML *Drosophila* model based on the expression of a completely human BCR-ABL1 fusion protein[56]. We generated several stable transgenic fly lines to express BCR-ABL1 protein using the yeast *Gal4/UAS* transcriptional regulation system controlled by a gene promoter active in specific tissues and stages (*Gal4* drivers)[47]. BCR-ABL1 expression was firstly triggered with the *sevenlessGal4* (*sevGal4*) construct that drives high levels of expression in some but not all photoreceptors[57], producing a mild rough eye similar to the one observed by Fogerty[55] (Figure 9A-E). This suggests that BCR-ABL1 interferes with the eye development as described for the human/fly chimera. To drive BCR-ABL1 expression in more eye cells, we used the *glass multimer reporterGal4* (*gmrGal4*) driver, active in all cells committed to differentiation and located posteriorly to the morphogenetic furrow[52], the cell indentation crossing from posterior to anterior the eye primordium (Figure 9N,O). BCR-ABL1 expression in these cells produced a severe "glazed" eye phenotype (Figure 9F-J, 10A,B,H,I). The regular structure of the eye is almost completely lost: ommatidia, the functional units of the eye, fail to differentiate and are no more distinguishable. The eye is smaller, bar-shaped and misplaced extra sensory bristles appear in the dorsal region (Figure 9H-J). Western blot analysis demonstrated that the severity of the phenotype correlates with the amount and phosphorylation of BCR-ABL1 protein (Figure 9K-M), indeed the low BCR-ABL1 expression level observed in line 1M (Figure 9K-M) results in a very mild phenotype (Figure 9G). To better understand the origin of the phenotype, we analyzed the expression of the pan-neuronal and eye photoreceptor marker Elav[64] in eye imaginal discs expressing BCR-ABL1. The typical $Elav^{+}$ photoreceptor clusters (Figure 9P) are reduced in number and altered in BCR-ABL1 expressing flies and this correlates with the described defects of the eye ordered structure (Figure 9P-T). To assess if the phenotype depends on the BCR-ABL1 kinase activity, we generated transgenic flies to express a kinase-dead mutant BCR-ABL1. *gmrGal4* driven

expression of the mutant protein does not affect eye development, indicating that BCR-ABL1 phenotype requires the enzymatic activity of the oncoprotein (Figure 10A-C,H).

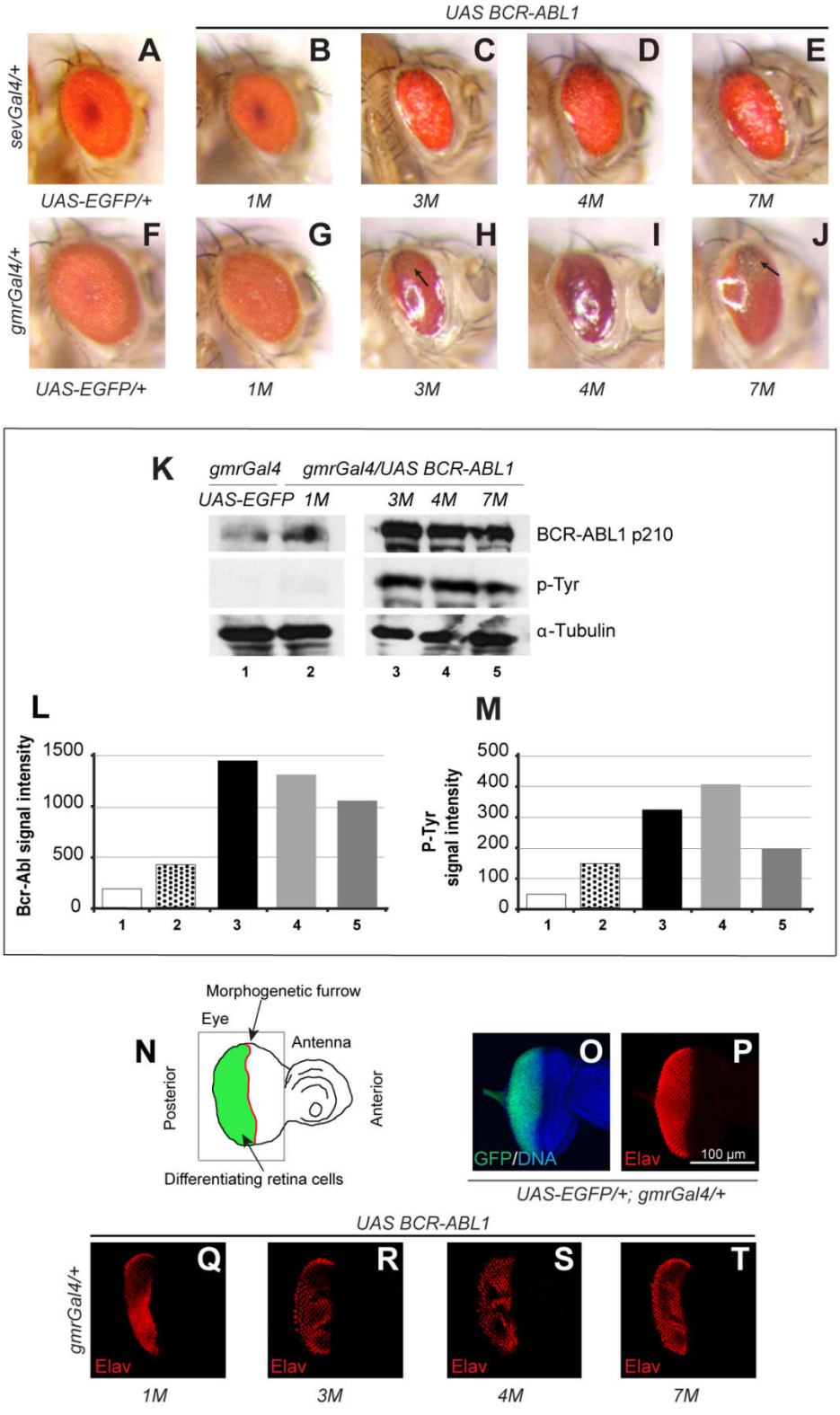

Figure 9. BCR-ABL1 expression in the developing eye cells affects photoreceptor differentiation. (**A-E**) Adult eyes expressing EGFP (**A**) or BCR-ABL1 in four independent transgenic lines: 1M (**B**), 3M (**C**), 4M (**D**), 7M (**E**) in a subset of differentiating photoreceptor cells under the control of the *sevenlessGal4* driver construct. High level of BCR-ABL1 (**C-E**) induces a "rough" eye phenotype due to impairment of cell differentiation. (**F-J**) Adult eyes expressing EGFP (**F**) or BCR-ABL1 (**G-J**) in all differentiating eye cells under the control of the *gmrGal4* driver construct. BCR-ABL1 expressed at high level in all differentiating eye cells (**H-J**) profoundly disrupts ommatidia development inducing a "glazed" phenotype, depigmented area and the appearance of extra bristles (black arrows). (**K-M**) Quantification of BCR-ABL1 expression (**K,L**) and tyrosine-phosphorylation (**K,M**) in protein extracts from adult heads of flies expressing either EGFP (lane 1) or BCR-ABL1 in independent transgenic fly lines (lanes 2-5). The protein extracts have been probed with antibodies raised against BCR, phosphorylated tyrosine residues (p-Tyr) or α–Tubulin as loading control. (**N**) Schematic of the eye-antenna imaginal disc from a late third instar larva; the positions of the eye and antenna primordia and of the morphogenetic furrows are indicated. The eye imaginal disc area posterior to the morphogenetic furrow and made of cells committed to terminal differentiation is indicated in green. The thin black square indicates the region of interest shown in panels O-T. (**O,P**) Eye imaginal disc from wild type late third instar larvae expressing EGFP under the control of the *gmrGal4* driver in cells posterior to the morphogenetic furrow and expressing the pan neuronal marker Elav in cells committed to terminal differentiation. (**Q-T**) Elav expression in eye imaginal discs from third instar larvae of the four independent transgenic lines that express BCR-ABL1 under the control of the *gmrGal4* driver construct. BCR-ABL1 expression reduces the number of differentiated photoreceptor as indicated by decrease of Elav expressing cells.

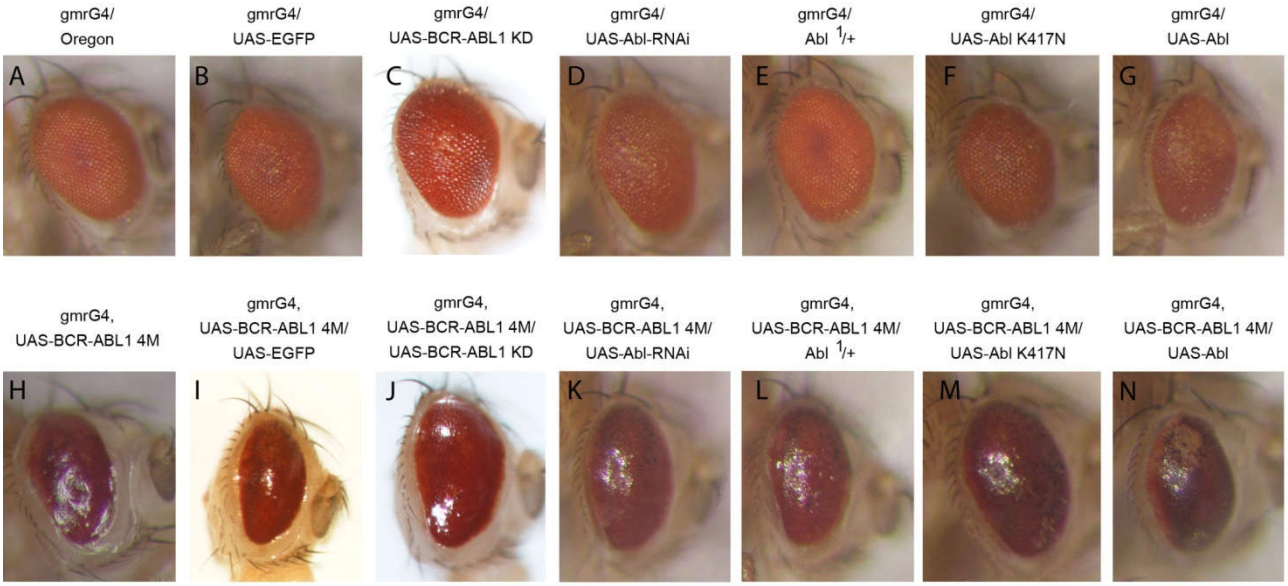

Figure 10. Adult eyes representative of the most frequent phenotypic class in the analysis of animals carrying the indicated genotypes and concerning the data included in Figure 2B.

4.2 Expression of human BCR-ABL1 interferes with eye development by altering dAbl *signaling*

To better understand the consequences of BCR-ABL1 overexpression in the eye, we investigated if the human oncoprotein could activate the endogenous pathway regulated by the *Drosophila* Abl kinase (dAbl). To quantify the phenotype we classified BCR-ABL1 eyes (line 4M) in three

phenotypic classes. Class 0 represents the most frequent "glazed" phenotype; class +1 is less severe: the eye is bigger and more prominent, and some ommatidia can be observed; class -1 is more severe, characterized by a less differentiated eye with evident lack of pigmentation in the most posterior region (Figure 11A). Interestingly, phenotype expressivity does not change comparing *gmrGal4,UAS-BCR-ABL1 4M* animals with *gmrGal4,UAS-BCR-ABL1 4M;UAS-EGFP* (Figure 11B, 10H,I) indicating that a single *gmrGal4* copy does not express a Gal4 limiting amount that could be titrated by increasing the number of UAS sequences. Since overexpression of dAbl (*UAS-Abl)* induces a very mild rough eye phenotype (Figure 10A,B,G), we investigated if it could enhance the BCR-ABL1 phenotype. We observed a worsening of the phenotype: all of the eyes belong to class -1, showing smaller eyes and more evident loss of pigmentation (Figure 11B, 10G,H,N). Then we investigated if *dAbl* loss of function (LOF) could suppress the BCR-ABL1 phenotype. *gmrGal4,UAS-BCR-ABL1 4M* animals heterozygous for a *dAbl* hypomorphic recessive lethal allele (Abl^{1}/+) showed a very mild phenotypic suppression but were not statistically different from the control (Figure 11B, 10E,H,L). However, *dAbl* downregulation through RNAi (*Abl-RNAi*) or expression of a dominant negative kinase-defective dAbl (*UAS-*Abl^{K417N}) induced a significant suppression of the BCR-ABL1 phenotype (Figure 11B, 10D,F,H,I,K,M). Interestingly, we observed that animals expressing either *Abl-RNAi* or *UAS-Abl* or *UAS-*Abl^{K417N} showed a similar mild disorganization of the ommatidia (Figure 10A,B,D,F,G) suggesting that the pathway activated by dAbl is indeed implicated in eye development. Furthermore, the genetic interactions between BCR-ABL1 expression and *dAbl* loss or gain of function suggest that dAbl, $dAbl^{K417N}$ and overexpressed BCR-ABL1 could compete for common binding targets. To confirm that BCR-ABL1 overexpression affects eye development by altering dAbl signaling cascade, we analyzed if BCR-ABL1 could functionally interact with components of the dAbl pathway. In detail, we focused on four genes whose LOF mutations genetically interact with a *dAbl* mutant phenotype.

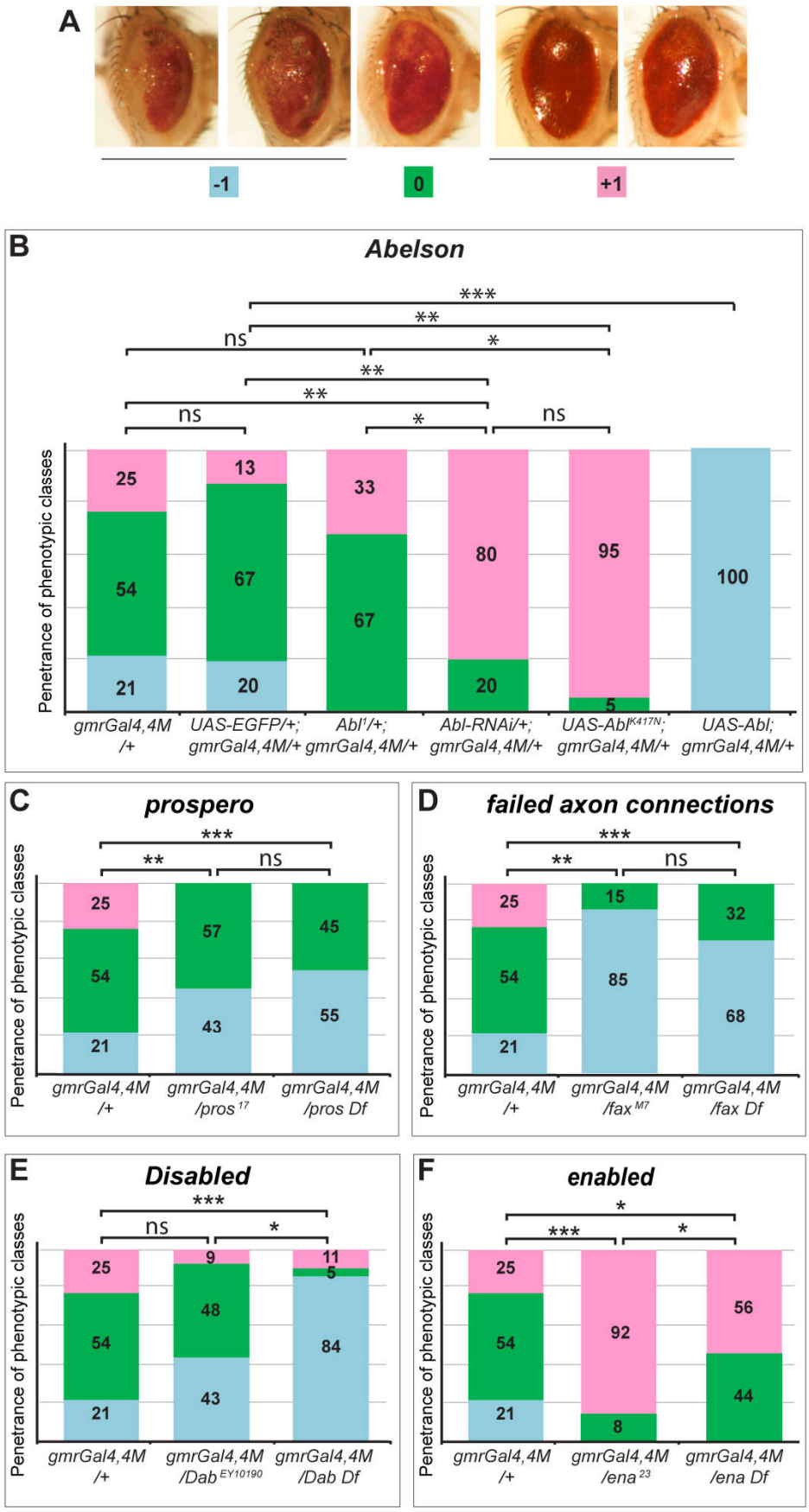
A
-1
0
+1
B
Abelson
Penetrance of phenotypic classes
gmrGal4,4M /+
UAS-EGFP/+; gmrGal4,4M/+
Abl1/+; gmrGal4,4M/+
Abl-RNAi/+; gmrGal4,4M/+
UAS-AblK417N; gmrGal4,4M/+
UAS-Abl; gmrGal4,4M/+
C
prospero
gmrGal4,4M /pros17
gmrGal4,4M /pros Df
D
failed axon connections
gmrGal4,4M /fax M7
gmrGal4,4M /fax Df
E
Disabled
gmrGal4,4M /Dab EY10190
gmrGal4,4M /Dab Df
F
enabled
gmrGal4,4M /ena 23
gmrGal4,4M /ena Df

Figure 11. BCR-ABL1 expression affects ommatidia development by altering the dAbl signaling pathway. (**A**) Adult eyes showing the phenotypic classes used to quantify the severity of the variable phenotype due to BCR-ABL1 expression in eye cells committed to terminal differentiation. Posterior is on the left. Class 0 (green): corresponds to the average phenotype shown by *gmrGal4, UAS-BCR-ABL1 4M* flies; the ommatidia are almost totally absent, the eye depigmented region is very small and the eye appears more flat than wild type. Class -1 (pale blue): corresponds to more severe phenotypes: the eyes are even more flat than class 0 eyes and the depigmented area is enlarged including a dorso-ventral sector in most posterior region of the eye. Class +1 (pink): corresponds to less severe phenotypes: few ommatidia are visible, the eyes are more bulging and the depigmented area is absent indicating improved eye cells differentiation. **(B-F)** Adult eyes from flies of the indicated genotypes have been classified to evaluate the frequency of the three phenotypic classes. (**B**) Piled histogram chart reporting the frequency of the different phenotypic classes in flies expressing BCR-ABL1 (*gmrGal4,4M/+*), coexpressing BCR-ABL1 and the EGFP (*UAS-EGFP/+;gmrGal4,4M/+*), expressing BCR-ABL1 but having a partial loss of the endogenous *Abl* gene trough the heterozygous Abl^{1} mutation (Abl^{1}*/+;gmrGal4,4M/+*), RNAi targeting *Abl* (*Abl-RNAi/+;gmrGal4,4M/+*), expression of a dominant negative dAbl mutant ($UAS\text{-}Abl^{K417N}$*;gmrGal4,4M/+*) or overexpression of the wild type Abl protein (*UAS-Abl;gmrGal4,4M/+*). (**C-F**) Piled histogram charts reporting the frequency of the three phenotypic classes in flies expressing BCR-ABL1 (*gmrGal4,4M*) and heterozygous for a loss of function allele or for a deletion of genes that behave as genetic modifiers of the embryonic lethality due to *Abl* LOF: *prospero* (**C**), *failed axon connection* (**D**), *Disable* (**E**) and *enable* (**F**). The statistic comparisons represent Mann-Whitney test (**P*<0.05, ***P*<0.01, ****P*<0.001).

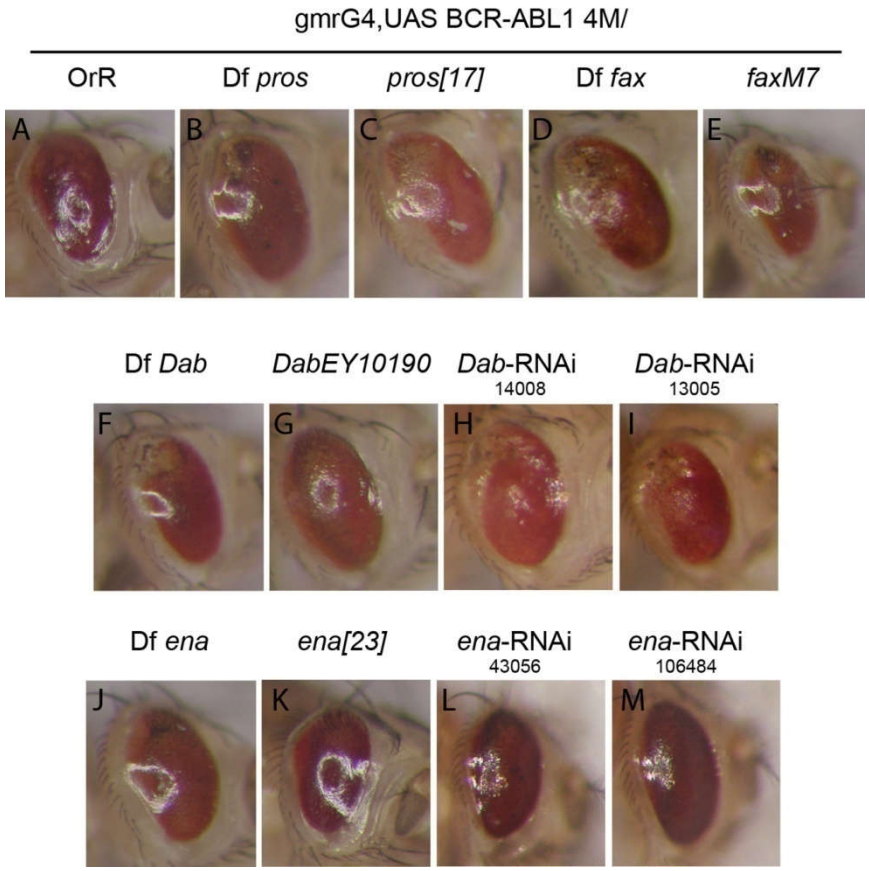

Figure 12. Adult eyes representative of the most frequent phenotypic class in the analysis of animals carrying the indicated genotypes and concerning the data included in Figure 2C-F, Figure 3A and Figure 5A.

Mutations of *prospero* (*pros*), a transcription factor that regulates neuronal differentiation[65], *failed axon connections* (*fax*), implicated both in neurogenesis and axonogenesis[66] and *Disabled* (*Dab*) that regulates cellular localization of dAbl[67], enhance the mutant *dAbl* phenotype. Moreover, *enabled* (*ena*) gene mutations suppress a *dAbl* mutant phenotype[68]. Interestingly, we found that either a deletion or a mutant allele of *pros* (Figure 11C, 12A-C) and *fax* (Figure 11D, 12A,D,E) were able to enhance the BCR-ABL1 phenotype. Moreover, although the insertional $Dab^{EY10190}$ allele did not change significantly the BCR-ABL1 phenotype, a deletion uncovering the *Dab* locus enhanced it (Figure 11E, 12A,F,G), confirming that BCR-ABL1 expression alters eye development likely by interacting with components of the dAbl pathway.

4.3 BCR-ABL1 expression increases phosphorylation of the dAbl substrate Ena

A genetic screen had previously identified an *ena* LOF allele as suppressor of the recessive lethality due to *dAbl* LOF mutations[68]. Ena is a cytoskeletal regulator that facilitates actin polymerization[69]. Its cellular localization depends on dAbl[68,70,71] and it is phosphorylated by both human and *Drosophila* Abl[72,73]. Heterozygosis of a LOF *ena* allele or of an *ena* deletion suppresses the BCR-ABL1 phenotype (Figure 11F, 12A,J,K). *ena* silencing with two independent constructs (*ena-RNAi)*, induces size increase and strong decrease of depigmented tissue in eyes expressing BCR-ABL1 (Figure 13A, 12A,L,M). Consistently, the analysis of Elav expression highlighted a more correct organization of photoreceptor clusters (Figure 13B-E). Furthermore, we looked at tyrosine-phosphorylation of the endogenous Ena. Flies expressing BCR-ABL1 showed increased levels of Ena tyrosine-phosphorylation (Figure 13F,H) even after Ena immunoprecipitation (Figure 13G,H) suggesting that Ena might be phosphorylated by BCR-ABL1. Taken together our data indicate that alteration of several components of dAbl pathway could be important for the mechanism by which BCR-ABL1 overexpression affects eye development, likely phosphorylating conserved targets in fly eye cells.

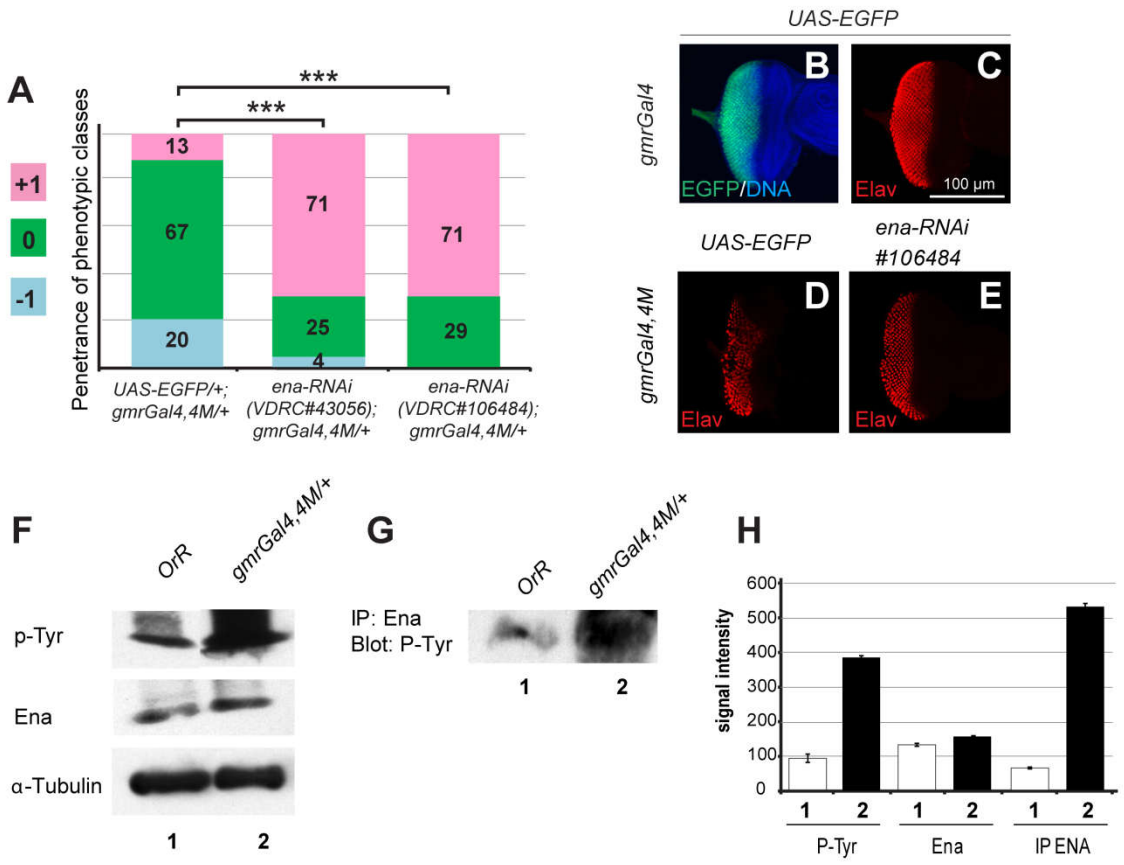

Figure 13. Ena LOF suppresses the eye phenotype due to BCR-ABL1 expression that increases phosphorylation of the dAbl target Ena. (**A**) Piled histogram chart reporting the frequency of the three phenotypic classes in flies coexpressing BCR-ABL1 (*gmrGal4,4M*) and EGFP (*UAS-EGFP/+;gmrGal4,4M/+*), or one of two independent *ena*-RNAi lines (VDRC#43056, VDRC#106484). (**B,C**) Eye imaginal discs from wild type late third instar larvae expressing EGFP under the control of the *gmrGal4* driver in cells posterior to the morphogenetic furrow (**B**) and expressing the pan neuronal marker Elav in cells committed to terminal differentiation (**C**). (**D,E**) Elav expression in eye imaginal discs from late third instar larvae expressing BCR-ABL1 (**D**) or larvae coexpressing BCR-ABL1 and *ena-RNAi* (**E**) under the control of the *gmrGal4* driver construct. BCR-ABL1 expression reduces the number of differentiated photoreceptors as indicated by decrease of Elav expressing cells and *ena* downregulation suppresses this phenotypic trait. (**F-H**) Quantification of Ena expression and tyrosine-phosphorylation in protein extracts (**F**) or Ena-immunoprecipitated proteins (**G**) from adult heads of flies expressing either EGFP (lane 1) or BCR-ABL1 (lane 2). Independent loads of equal amount of protein extracts or Ena-immunoprecipitated proteins have been probed with antibodies raised against phosphorylated tyrosine residues (p-Tyr), Ena or α–Tubulin as loading control. (**H**) Average signal intensity from replica of the experiment shown in F and G. Ena immunoprecipitation and probing for tyrosine-phosphorylation confirmed the increase of Ena tyrosine-phosphorylation in animals expressing BCR-ABL1. The statistic comparisons in panel **A** represent Mann-Whitney test (**P*<0.05, ***P*<0.01, ****P*<0.001).

4.4 A component of the BCR-ABL1 activated pathway in human leukemia modulates the eye phenotype in Drosophila

To further assess the effectiveness of the model, we investigated if *Drosophila* homolog of a gene known to be involved in BCR-ABL1 signaling in human leukemia was also able to modulate the BCR-ABL1 phenotype. Signal Transducer and Activator of Transcription 5 (STAT5) is a transcription factor activated in response to cytokines and its role in malignant transformation is well established[74]. Several studies showed that BCR-ABL1 induces phosphorylation and constitutive activation of STAT5, hindering apoptosis in leukemic cells[75]. The JAK/STAT pathway is required during *Drosophila* eye morphogenesis and larval hematopoiesis[76,77]. Interestingly, loss of *STAT92E* function ($STAT92E^{06346}$), the fly counterpart of STAT5, induced a strong suppression of BCR-ABL1 phenotype (Figure 14, 15A,B). Flies coexpressing a STAT dominant negative allele ($STAT^{DN}$) and BCR-ABL1 showed an even weaker phenotype (Figure 14A, 15A,C) confirming that STAT is involved in BCR-ABL1 activated pathway in *Drosophila* eye.

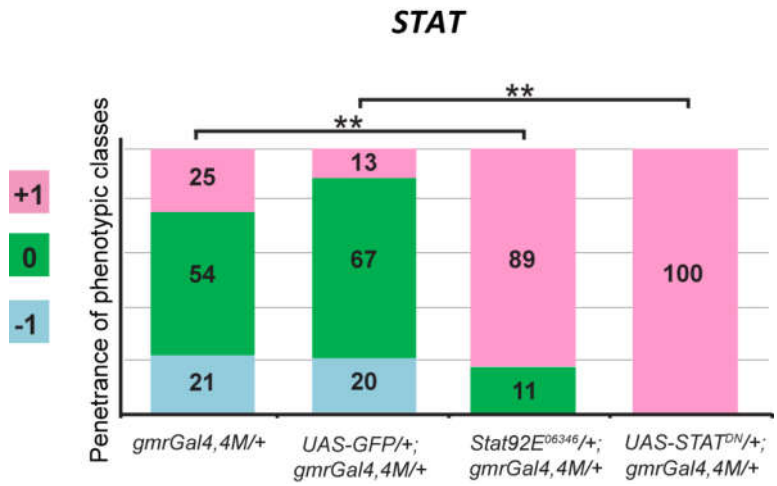

Figure 14. A component of the BCR-ABL1 activated *pathway* in human leukemia, modulate the eye phenotype in *Drosophila*. Piled histogram chart reporting the frequency of the three phenotypic classes in flies expressing BCR-ABL1 (*gmrGal4,4M*) and heterozygous for a loss of function $STAT92E^{06346}$ allele or overexpressing a dominant negative allele $STAT^{DN}$. Function reduction of STAT, a gene encoding the homolog of the STAT5 protein involved in the BCR-ABL1 activated pathway in human leukemia cells, suppresses the BCR-ABL1 dependent phenotype in the fly eye. The statistic comparisons represent Mann-Whitney test (*P<0.05, **P<0.01, ***P<0.001).

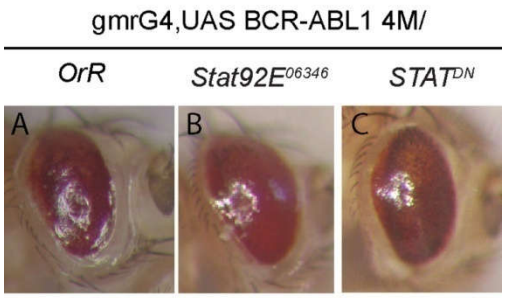

Figure 15. Adult eyes representative of the most frequent phenotypic class in the analysis of animals carrying the indicated genotypes and concerning the data included in Figure 4.

4.5 The human homologs of Disabled, Dab1 and Dab2 are altered in CML patients

To better explore the efficacy of the model we analyzed the *Disabled* gene that encodes for an adaptor protein acting downstream of many receptor tyrosine kinases (RTK)[65,78]. In the embryo *Dab* LOF disrupts the intracellular localization of dAbl and consequently that of phosphorylated Ena and F-Actin accumulation[79]. In the fly eye we observed an enhancement of BCR-ABL1 phenotype in animals heterozygous for a *Dab* deletion. Thus, we further reduced *Dab* function by gene silencing. Interestingly, two independent RNAi lines worsened the BCR-ABL1 phenotype more than *Dab* deletion (Figure 11, 16, 12A,F-I): most of the eyes were smaller and showed depigmented scar-like tissue (Figure 12A,F,H,I). Consistently, alterations of the ommatidia clusters, revealed by Elav expression, worsened compared to control (Figure 16B-E). To establish if Dab might have a role in CML we analyzed the 2 human counterparts of *Disabled*, *Dab1* and *Dab2* in human primary cells. *Dab1* is a large common fragile site gene and the Dab1 protein acts as signal transducer that interacts with many RTK pathways[80]. *Dab2* encodes for an adaptor protein implicated in growth factor signaling, endocytosis, cell adhesion, hematopoietic cells differentiation and cell signaling of various RTKs[81]. The expression of both genes is often decreased in many human solid cancers, suggesting their possible role in oncogenesis[80,82].

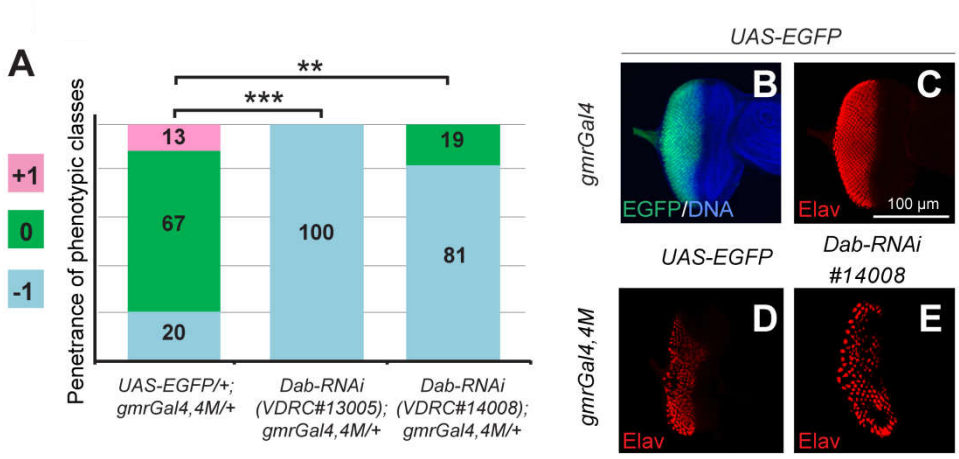

Figure 16. *Dab* downregulation enhances the eye phenotype due to BCR-ABL1. (**A**) Piled histogram chart reporting the frequency of the three phenotypic classes in flies coexpressing BCR-ABL1 (*gmrGal4,4M*) and EGFP (*UAS-EGFP/+;gmrGal4,4M/+*), or one of two independent *Dab-RNAi* constructs (VDRC#13005, VDRC#14008). (**B,C**) Eye imaginal discs from wild type late third instar larvae expressing EGFP under the control of the *gmrGal4* driver in cells posterior to the morphogenetic furrow and expressing the pan neuronal marker Elav in cells committed to terminal differentiation. (**D,E**) Elav expression in eye imaginal discs from late third instar larvae expressing BCR-ABL1 (**D**) or larvae coexpressing BCR-ABL1 and *Dab*-RNAi (**E**) under the control of the *gmrGal4* driver construct. BCR-ABL1 expression reduces the number of differentiated photoreceptors as indicated by decrease of Elav expressing cells and *Dab* downregulation enhances this phenotypic trait. The statistic comparisons represent Mann-Whitney test (**P*<0.05, ***P*<0.01, ****P*<0.001).

Interestingly, qRT-PCR analysis revealed a significant downregulation of both genes in CML patients at diagnosis compared to controls either in peripheral blood (PB) or in bone marrow (BM) samples (Figure 17A,G). Analysis of BM samples from CML patients during molecular remission (MR) showed increased levels of expression of both *Dab1* (Figure 17B) and *Dab2* (Figure 17H) with respect to patients with primary resistance to TKI (Resistant Pts). Moreover, immunofluorescence assays demonstrated a significant down-modulation of both proteins in PB samples at diagnosis compared to controls or MR patients (Figure 17C,D,I,J). Finally, transfection experiments in K562 cells using a plasmid carrying the whole *Dab1* coding sequence, demonstrated that reactivation of Dab1 expression reduced cell proliferation (Figure 17E,F).

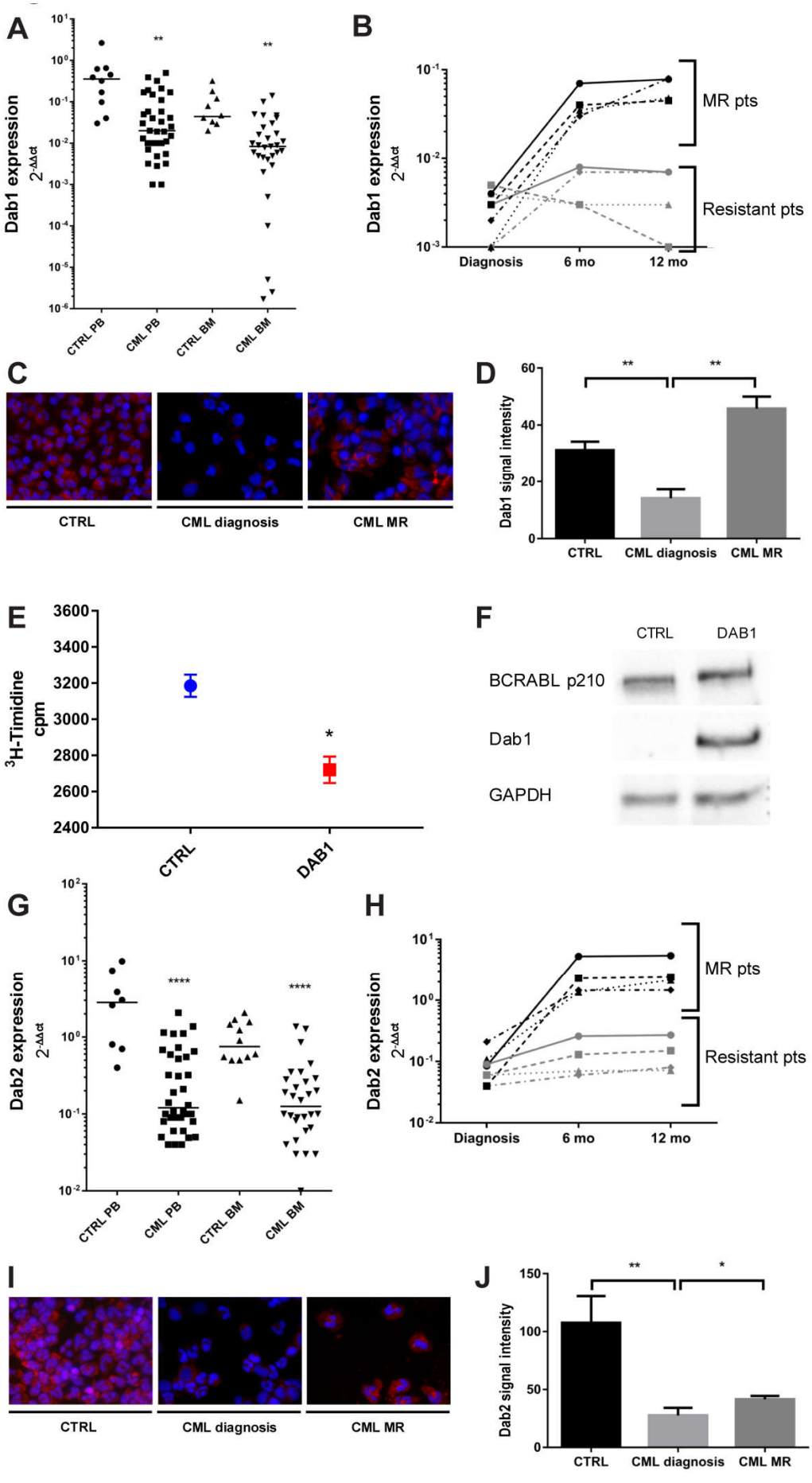
A
Dab1 expression
2-ΔΔct
CTRL PB
CML PB
CTRL BM
CML BM
B
Dab1 expression
2-ΔΔct
MR pts
Resistant pts
Diagnosis
6 mo
12 mo
C
CTRL
CML diagnosis
CML MR
D
Dab1 signal intensity
CTRL
CML diagnosis
CML MR
E
3H-Timidine
cpm
CTRL
DAB1
F
CTRL
DAB1
BCRABL p210
Dab1
GAPDH
G
Dab2 expression
2-ΔΔct
CTRL PB
CML PB
CTRL BM
CML BM
H
Dab2 expression
2-ΔΔct
MR pts
Resistant pts
Diagnosis
6 mo
12 mo
I
CTRL
CML diagnosis
CML MR
J
Dab2 signal intensity
CTRL
CML diagnosis
CML MR

Figure 17. Altered expression pattern of the human *Disabled* homologs, *Dab1* and *Dab2,* in CML patients. (**A**) Down-regulation of *Dab1* RNA expression in CML patients compared to healthy donors. In particular we found 1 log of reduction of *Dab1* expression both in PB ($P<0.01$) and in BM ($P<0.01$) (median values $2^{-\Delta\Delta ct}$: 0.02 *vs* 0.3 in PB and 0.008 *vs* 0.04 in BM). (**B**) Expression pattern of *Dab1* in CML patients during Molecular Remission (MR) compared to resistant patients. (**C**) Immunofluorescence staining of Dab1 protein (red) in PB samples of healthy donors, CML patients at diagnosis and CML patients during MR. Nuclei are stained in blue. (**D**) Quantification of Dab1 protein expression in the immunofluorescence assay. (**E**) ^{3}H-Timidine proliferation assay showing a 20% reduction of cell proliferation in K562 cells transfected with *Dab1* plasmid compared to control. (**F**) Western blot of protein extracts from K562 cells transfected with an empty vector (lane 1) and transfected with a *Dab1* expression vector (lane 2), showing detectable expression of Dab1 only in K562 cells transfected with the *Dab1* vector. Independent loads of equal amount of protein extract have been probed with antibodies raised against BCR, Dab1 and GAPDH as loading control (**G**) Down-regulation of *Dab2* RNA expression in CML patients compared to healthy donors. In particular *Dab2* expression was found statistically decreased ($P<0.0001$ and $P<0.0001$ in PB and BM respectively) with median values of 0.12 *vs* 2.8 and 0.12 *vs* 0.7 in PB and BM respectively. (**H**) Expression pattern of *Dab2* in CML patients during MR compared to resistant patients. (**I**) Immunofluorescence staining of Dab2 protein (red) in PB samples of healthy donors, CML patients at diagnosis and CML patients during MR. Nuclei are stained in blue. (**J**) Quantification of Dab2 protein expression in immunofluorescence assay. The statistic comparisons represent Student's t test (*$P<0.05$, **$P<0.01$, ****$P<0.0001$). Error bars indicate s.e.

4.6 BCR-ABL1 expression impairs Drosophila blood cell homeostasis

To further confirm the efficacy of the model, we investigated the effects of BCR-ABL1 expression in the Lymph Gland (LG), the hematopoietic organ of the larva. The LG begins to develop in the embryo[83] and grows up from multipotent progenitor cells (prohemocytes) that proliferate and enter a quiescence phase during the second instar (L2). During the third instar (L3) some prohemocytes start again to proliferate and differentiate. The LG breaks apart at the beginning of metamorphosis releasing differentiated blood cells (hemocytes) into the hemolymph, the *Drosophila* blood[84,85]. During the L3, three functional regions can be distinguished in the LG[86]: the medullary zone (MZ), populated by prohemocytes; the posterior signaling center (PSC) that regulates prohemocytes exit from quiescence; the cortical zone (CZ), made up of differentiating hemocytes[87,88]. Breaking up of LG can happen prematurely in late-L3 if the number of differentiating hemocyte increases. As reaction to excessive hematopoiesis, the hemocytes aggregate and a spontaneous melanisation process takes place inducing the formation of melanotic nodules[63,85,89,90]. Constitutive BCR-ABL1 expression under the control of *domelessGal4* (*domeGal4*) driver, active in the MZ of the lymph gland[58,63] is lethal (data not shown). To

overcome this problem, we repressed expression of BCR-ABL1 by coexpressing a heat sensitive mutant of the Gal4 repressor Gal80 (*tubGal80^{TS}*) until larvae reached the desired instar (TARGET system)[61]. While BCR-ABL1 expression from the first instar (L1) induced lethality (data not shown), expression from the L2 allowed larvae to survive and to develop melanotic nodules at L3 (Figure 18A,B). This suggests that BCR-ABL1 expression in the MZ precursors might induce increase of circulating hemocytes (Figure 18C). When compared to control (Figure 18A), 45% of *domeGal4,BCR-ABL1 3M,tubGal80^{TS}* larvae showed 2 to 3 small melanotic nodules (Figure 18B,C). This correlates with an increased number of circulating hemocytes in hemolymph preparations (Figure 18D). BCR-ABL1 expression starting from the early-L3 did not show any significant phenotype (Figure 18C), indicating that only when BCR-ABL1 is expressed when prohemocytes enter quiescence it is able to increase hematopoiesis. Consistently, constitutive expression of the kinase-dead mutant *BCR-ABL1^{KD}* did not induce any significant phenotype (Figure 18C). Since *dAbl* as *Dab* and *ena* are expressed in the lymph gland[91], we assessed whether decreased *dAbl* function is able to rescue the phenotype. We coexpressed BCR-ABL1 and *Abl-RNAi*, and observed a significant decrease of the phenotype penetrance (Figure 18E). Then, we investigated if *Dab* or *ena* downregulation genetically interact with BCR-ABL1 expression also during hematopoiesis. *Dab-RNAi* in the MZ starting from L2 was able to enhance the melanotic nodule phenotype, inducing a significant increase of the penetrance (Figure 18F). Consistently, larvae coexpressing *Dab* (*UAS-Dab*) and BCR-ABL1 in the MZ starting from L2 showed phenotypic suppression (Figure 18F). Moreover, *ena-RNAi* weakly suppressed BCR-ABL1 phenotype (Figure 18G) decreasing the phenotype penetrance. As a control, we did not observe any phenotype due to *Dab* or *ena* downregulation or *Dab* overexpression in prohemocytes (Figure 18F,G).

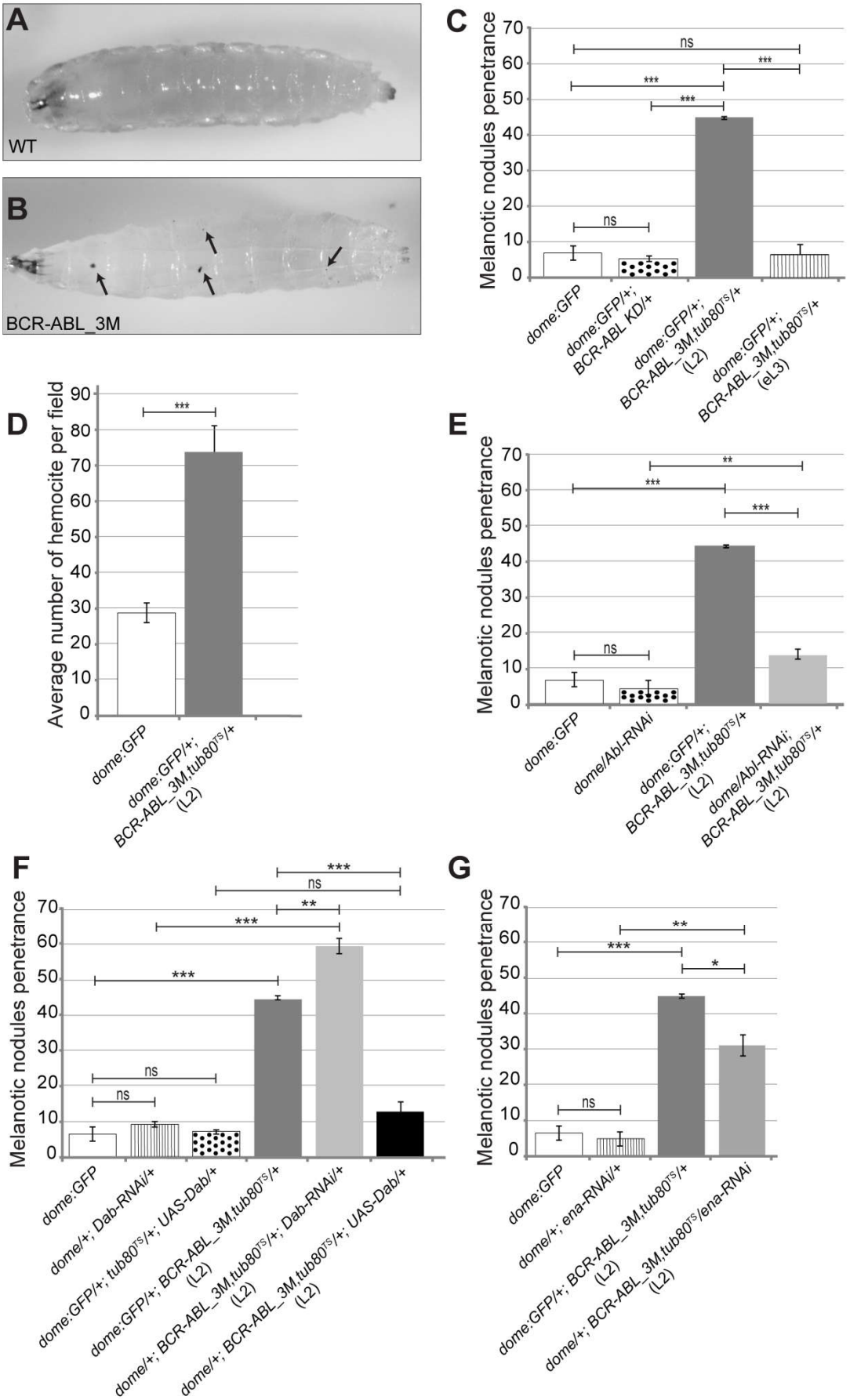
A
WT
B
BCR-ABL_3M
C
Melanotic nodules penetrance
ns
***
dome:GFP
dome:GFP/+; BCR-ABL KD/+
dome:GFP/+; BCR-ABL_3M,tub80TS/+ (L2)
dome:GFP/+; BCR-ABL_3M,tub80TS/+ (eL3)
D
Average number of hemocite per field
dome:GFP
dome:GFP/+; BCR-ABL_3M,tub80TS/+ (L2)
E
Melanotic nodules penetrance
**
dome/Abl-RNAi
dome:GFP/+; BCR-ABL_3M,tub80TS/+ (L2)
dome/Abl-RNAi; BCR-ABL_3M,tub80TS/+ (L2)
F
Melanotic nodules penetrance
dome/+; Dab-RNAi/+
dome:GFP/+; tub80TS/+; UAS-Dab/+
dome:GFP/+; BCR-ABL_3M,tub80TS/+ (L2)
dome/+; BCR-ABL_3M,tub80TS/+; Dab-RNAi/+ (L2)
dome/+; BCR-ABL_3M,tub80TS/+; UAS-Dab/+ (L2)
G
Melanotic nodules penetrance
dome/+; ena-RNAi/+
dome:GFP/+; BCR-ABL_3M,tub80TS/+ (L2)
dome/+; BCR-ABL_3M,tub80TS/ena-RNAi (L2)

Figure 18. BCR-ABL1 expression in the hematopoietic precursor cells of the lymph gland impairs *Drosophila* blood cells homeostasis increasing the number of circulating blood cells. (**A**) A w^{1118} mid-L3 instar larva used as wild type control. (**B**) A mid-L3 larva conditionally expressing BCR-ABL1 in the hematopoietic precursors of the lymph gland Medullary Zone under the control of the *domelessGal4* driver construct (*dome:GFP/+;BCR-ABL1_3M,tub80TS/+*). BCR-ABL1 expression has been induced in staged L2 or early-L3 larvae by exposing the animals to 29°C during the indicated larval instars to disrupt the ability of the temperature sensitive Gal80 mutant to inhibit the Gal4 transactivation activity. Black arrows in **B** indicate melanotic nodules. Anterior is on the left. (**C**) Penetrance of the melanotic nodule phenotype in mid-L3 control larvae expressing GFP under the control of the *domelessGal4* driver *(domeGFP)*, in larvae constitutively expressing a kinase-dead BCR-ABL1 mutant protein (*dome:GFP/+;BCR-ABL1 KD/+*) and in larvae in which BCR-ABL1 (*dome:GFP/+;BCR-ABL1_3M,tub80TS/+*) expression has been induced starting from the L2 (L2) or from the early-L3 (eL3) instars. (**D**) Evaluation of the average number of hemocytes per field after bleeding of *dome:GFP/+;BCR-ABL1_3M,tub80TS/+* and *dome:GFP/+* larvae. BCR-ABL1 expression induces the appearance of melanotic nodules and this correlates with increase of circulating hemocytes. (**E**) Penetrance of the melanotic nodule phenotype in mid-L3 control larvae (*dome:GFP*), in larvae expressing *Abl-RNAi* (*dome/Abl-RNAi*), in larvae in which BCR-ABL1 alone (*dome:GFP/+;BCR-ABL1_3M,tub80TS/+*) or together with *Abl-RNAi* (*dome/Abl-RNAi;BCR-ABL1_3M,tub80TS/+*) are expressed from the L2 instar. (**F**) Penetrance of the melanotic nodule phenotype in mid-L3 control larvae (*dome:GFP*), in larvae expressing *Dab-RNAi* (*dome/+;Dab-RNAi/+*), in larvae conditionally expressing the Dab protein (*dome:GFP/+;tub80TS/+;UAS-Dab/+*), in larvae in which BCR-ABL1 alone (*dome:GFP/+;BCR-ABL1_3M,tub80TS/+*) or together with either *Dab-RNAi* (*dome/+;BCR-ABL1_3M,tub80TS/+;Dab-RNAi/+*) or *UAS-Dab* (*dome/+;BCR-ABL1_3M,tub80TS/+;UAS-Dab/+)* are expressed from the L2 instar. (**G**) Penetrance of the melanotic nodule phenotype in mid-L3 control larvae (*dome:GFP*), in larvae expressing *ena-RNAi* (*dome/+;ena-RNAi/+*), in larvae in which BCR-ABL1 alone (*dome:GFP/+;BCR-ABL1_3M,tub80TS/+*) or together with *ena-RNAi* (*dome/+;BCR-ABL1_3M,tub80TS/ena-RNAi*) are expressed from the L2 instar. The average phenotype penetrance is calculated from three independent experiments, each involving 15-95 larvae. The statistic comparisons represent Student's t test (**P*<0.05, ***P*<0.01, ****P*<0.001, ns=not significant). Error bars indicate s.e.

4.7 BCR-ABL1 induced phenotype was altered by some stocks of deletions

Using the recombinant fly carrying both the *gmrGal4* and the *UAS-BCR-ABL1* transgenes in cis on the 3rd chromosome (*gmrGal4,UAS-BCR-ABL1 4M/TM3*), we were able to perform a genetic screening of most of *Drosophila* genome (autosomes 2 and 3). This was performed by crossing the *BCR-ABL1* recombinant fly with more than 200 stocks of deletions (Figure 19, Table 2) covering approximately 10000 genes of *Drosophila*, and by classifying the changes of the resulting phenotype in 5 arbitrary classes: class 0 represent the average BCR-ABL1 phenotype; class +1 represent a milder phenotype, characterized by an improvement of either dimension or differentiation; class +2 represent the weakest phenotype, with an improvement in both dimension and differentiation with at least a partial rescue of phenotype; class -1 represent a stronger phenotype, characterized by a worsening of either dimension or differentiation; class -2 represent

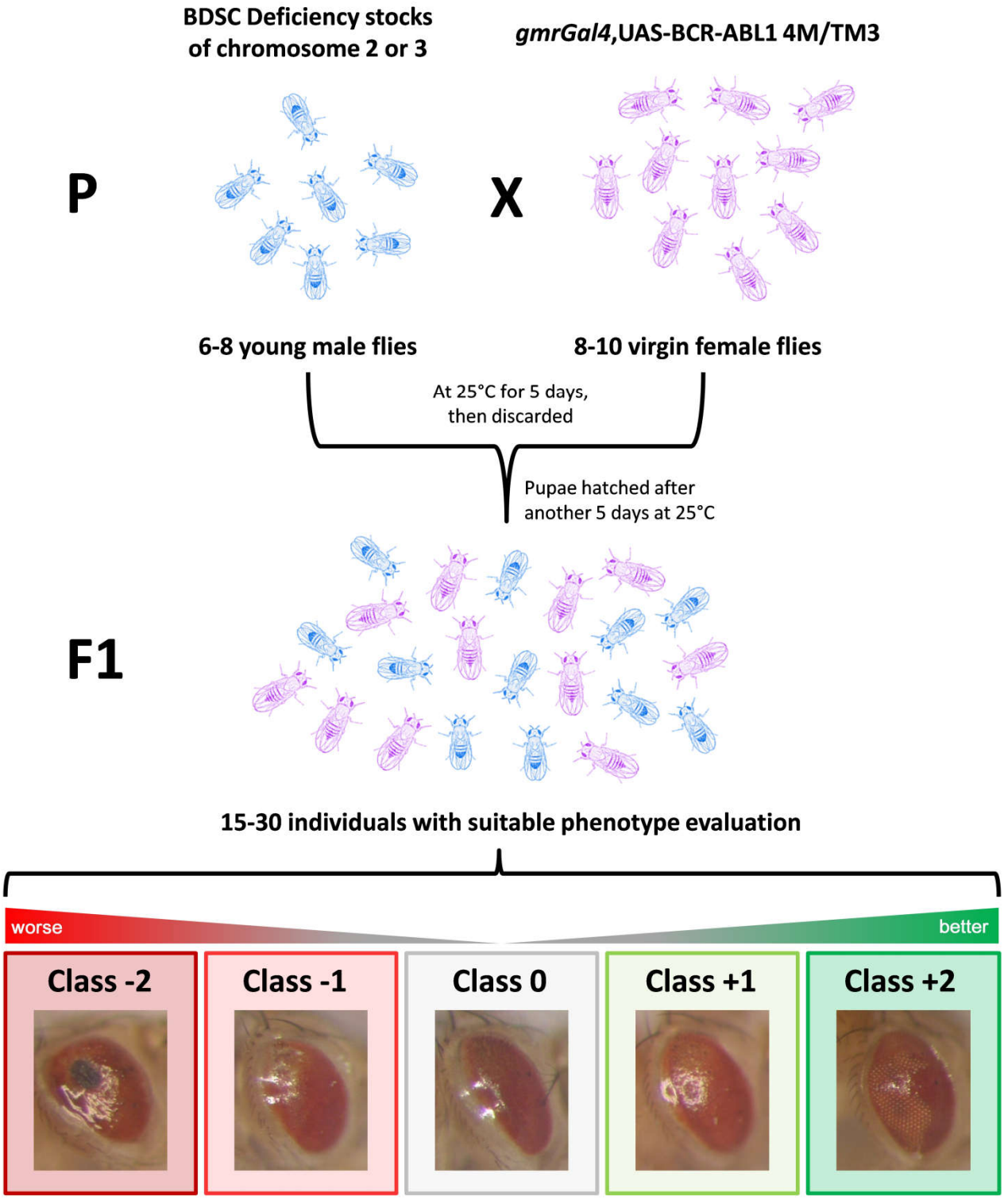

Figure 19. Typical crossing setup for BCR-ABL1 screening. Schematic view of crossing between male flies harboring deletions on chromosomes 2 and 3 and virgin female flies carrying BCR-ABL1 transgene expressed in the eyes of the animals (genotype *gmrGal4,UAS-BCR-ABL1 4M/TM3).* Typically, 6 to 8 young males are chosen from the deficiency stock and put together with 10 virgin females *gmrGal4,UAS-BCR-ABL1 4M/TM3* in a new tube (P generation), left at 25°C for 5 days, and then discarded. After another 5 days at 25°C pupae start hatching and 15-30 F1 generation individuals with the suitable phenotype are photographed and classified.

Chromosome arm	#	BDSC Stock #	Most represented phenotypic class	Chromosome arm	#	BDSC Stock #	Most represented phenotypic class	Chromosome arm	#	BDSC Stock #	Most represented phenotypic class
2L	1	3638	+1	2R	74	7875	+2	3L	147	6457	+1
	2	8672	+1		75	7876	-1		148	6755	-1
	3	6608	0		76	7896	-2		149	6964	0
	4	7144	-2		77	7414	0		150	3617	0
	5	6875	0		78	9596	-1		151	600	-1
	6	6283	+2		79	5680	+2		152	3124	-1
	7	3084	-1		80	5574	+1		153	3650	0
	8	6648	0		81	7441	0		154	6456	0
	9	1567	+1		82	1547	-1		155	7079	0
	10	6965	+2		83	6866	0		156	8082	+2
	11	3133	+2		84	6647	-2		157	8101	-1
	12	90	+2		85	3467	-2		158	2990	-1
	13	6507	+2		86	1007	+1		159	2608	+2
	14	5530	+1		87	1888	+1		160	3686	-2
	15	693	0		88	3368	+2		161	4366	0
	16	9270	0		89	1743	+1		162	4429	-1
	17	8835	0		90	1702	+1	3R	163	383	-2
	18	8674	0		91	442	-2		164	430	+2
	19	7497	Lethal		92	9496	-1		165	669	-2
	20	781	+1		93	6455	0		166	756	+1
	21	490	-1		94	3518	-1		167	823	0
	22	6299	+1		95	3520	+1		168	1842	-2
	23	6338	0		96	6779	0		169	1884	+1
	24	6374	-1		97	6780	0		170	1910	0
	25	2414	0		98	6609	0		171	1931	+1
	26	5420	+2		99	5246	0		172	1962	-2
	27	4956	+1		100	282	Lethal		173	1868	-2
	28	9502	+1		101	3909	Lethal		174	1990	+2
	29	140	0		102	7273	+1		175	2363	-1
	30	8836	+2		103	1682	0		176	2586	+2
	31	9298	+2		104	9691	0		177	3007	0
	32	2892	0		105	2604	+1		178	3011	+2
	33	6478	-1		106	9069	+2		179	3012	0
	34	8469	-1		107	2471	-1		180	1467	Not performed
	35	3366	+1		108	4961	0		181	1518	0
	36	9503	+1	3L	109	463	+2		182	1534	+1
	37	7142	0		110	997	0		183	2393	-1
	38	9505	-1		111	1420	-1		184	2425	-2
	39	5869	+1		112	2400	0		185	2585	+1
	40	3079	-1		113	1541	0		186	3128	Not performed
	41	6999	+2		114	2577	+1		187	3340	-1
	42	9506	+2		115	3096	+1		188	3468	-2
	43	1491	-2		116	3126	-2		189	3546	0
	44	420	-2		117	3127	-1		190	3547	+1
	45	567	+2		118	4506	+2		191	4431	-1
	46	179	+1		119	5126	0		192	4432	0
	47	7143	+1		120	5877	-1		193	4787	-1
	48	3588	+1		121	5951	0		194	4940	+2
	49	167	-1		122	6411	+1		195	4962	+1
	50	7531	+1		123	6551	0		196	5601	0
	51	9510	0		124	6646	0		197	5694	0
	52	4959	+2		125	6649	-2		198	7413	-2
	53	1045	0		126	2612	0		199	7623	Lethal
	54	9594	+2		127	3640	0		200	7681	+1
	55	7147	0		128	3649	+2		201	7682	-1
	56	3138	-1		129	4393	0		202	7990	0
	57	2583	0		130	5492	-1		203	7992	0
2R	58	739	-2		131	5878	0		204	8103	+2
	59	198	+1		132	6471	-1		205	8491	0
	60	201	+2		133	6754	+2		206	6756	+1
	61	4966	-2		134	6867	-2		207	7080	-1
	62	6917	+1		135	7566	-1		208	7412	-1
	63	9410	-1		136	439	-1		209	7443	-1
	64	190	-1		137	4430	-1		210	7674	0
	65	1145	0		138	6460	0		211	7675	-1
	66	3591	+1		139	9693	-1		212	7676	0
	67	7145	+1		140	9700	-2		213	1920	-2
	68	4960	0		141	23149	-1		214	8583	0
	69	7146	+1		142	23668	+2		215	9497	-2
	70	5879	-1		143	2052	-2		216	9500	+1
	71	754	+2		144	2611	+2		217	9529	+1
	72	7445	-1		145	3024	-1				
	73	6516	-1		146	4500	0				

Table 2. List of deficiency stocks for chromosomes 2 and 3 used in the screening and phenotype classification

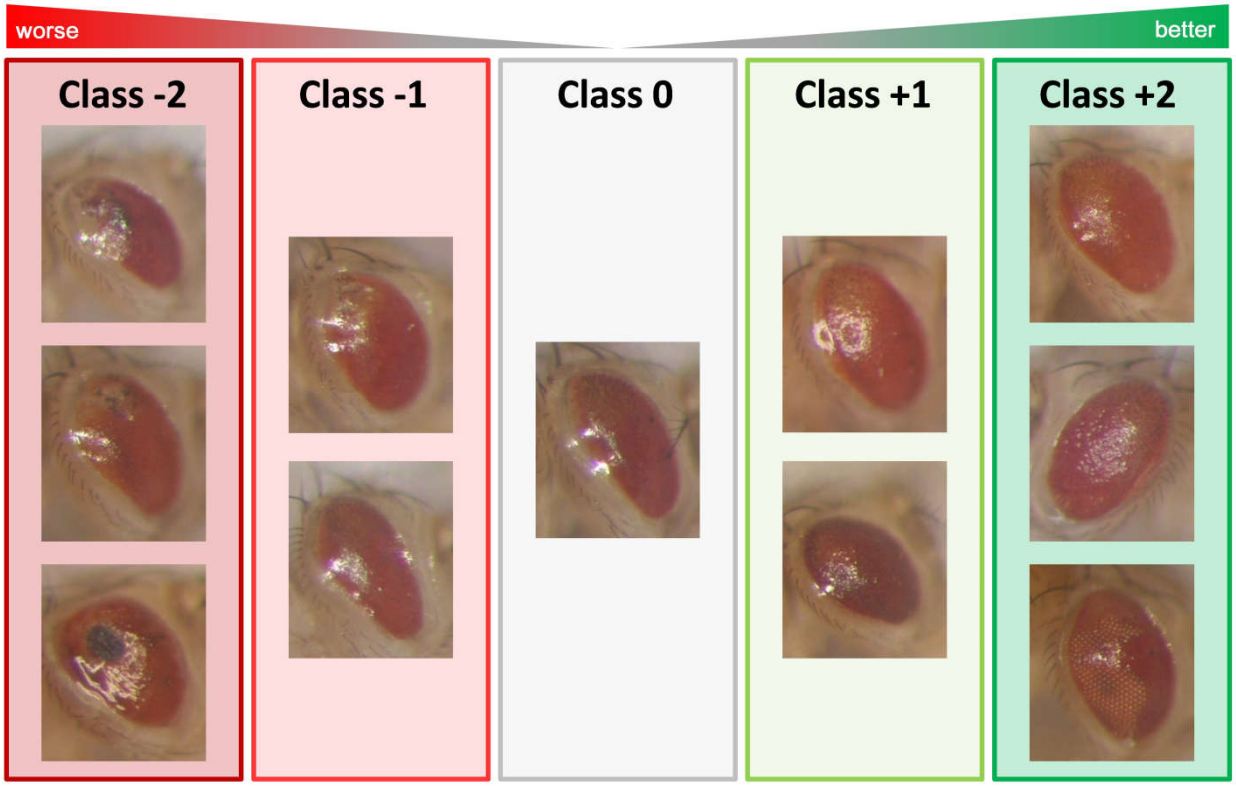

Figure 20. Classification of BCR-ABL1 phenotype modifications into five arbitrary classes. To quantify the phenotype, 15-30 F1 flies from three independent crosses with the suitable genotype, were classified into five arbitrary phenotypic classes. Class 0 (grey panel) represents the average phenotype of *gmrGal4,UAS-BCR-ABL1 4M* flies; class -1 (light red panel) represents a more severe eye phenotype and class -2 (dark red panel) the most severe eye phenotype (enhancement); class +1 (light green panel) represents a weaker phenotype and class +2 (dark green panel) represents the weakest phenotype (suppression).

the strongest phenotype, characterized by a worsening of both dimension and differentiation, the presence of necrosis areas and more misplaced extra-sensory bristles (Figure 19-20, Table 2). The eye phenotype is not always completely penetrant, but here we chose to report only the most represented class in each cross. Out of 217 stocks of deletions, we found a total of 58 major modifiers, 33 (16%) belonging to class +2 and 25 (12%) belonging to class -2. Furthermore, we found 90 minor modifiers, 43 (20%) classified as +1 and 47 (22%) as -1. A total of 63 stocks were classified as non modifiers (class 0, 30%) (Figure 21, Table 2). Finally 4 crosses resulted in lethality and 2 were not due to viability problems with the stocks of deletion. In particular, the 3rd chromosome accounted for the major presence of pejorative phenotypes (-2 and -1 classes): 43% in arm L and 38% in arm R with respect to chromosome 2, which accounted for 20 and 34% in L and

R, respectively. In addition, the chromosome 2L showed the maximal presence of ameliorative phenotype (+2 and +1 classes): 52% respect to 39% of 2R and 33% of 3L and 3R, respectively (Figure 21, Table 2).

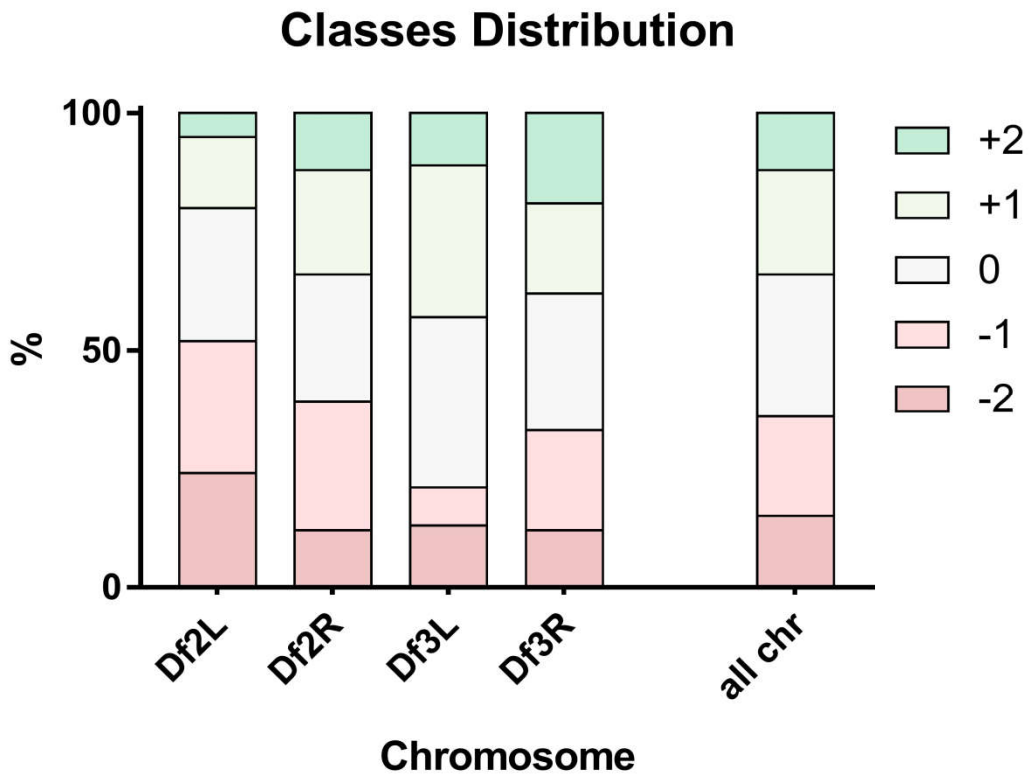

Figure 2. Phenotypic classes distribution on chromosomes arms. Schematic representation of the distribution of phenotype modifications among the four chromosome arm deficiency kits analyzed, (Df2L, Df2R, Df3L, Df3R). The last column shows the sum of all deficiencies analyzed.

After unaffected/contrasted phenotype genes cleaning, as indicated in methods, all results were sorted by biological process gene ontology (GO) and results were summarized in Supplementary Table 1. The GO classes with better stock/genes frequency for the ameliorative (7 stock with +1 or +2 vs 0 with -1 or -2 classes) and pejorative phenotype (0 stock with +1 or +2 vs 6 with -1 or -2 classes) are shown in Figure 22 and Table 3. Interestingly, in some of these GO families, genes identified in more than one stock are present, as for examples FBgn0003892, included in all ameliorative top classes and identified in two different stock (#201 and #198), or FBgn0015790, included in two pejorative stocks (#2425 and #3340).

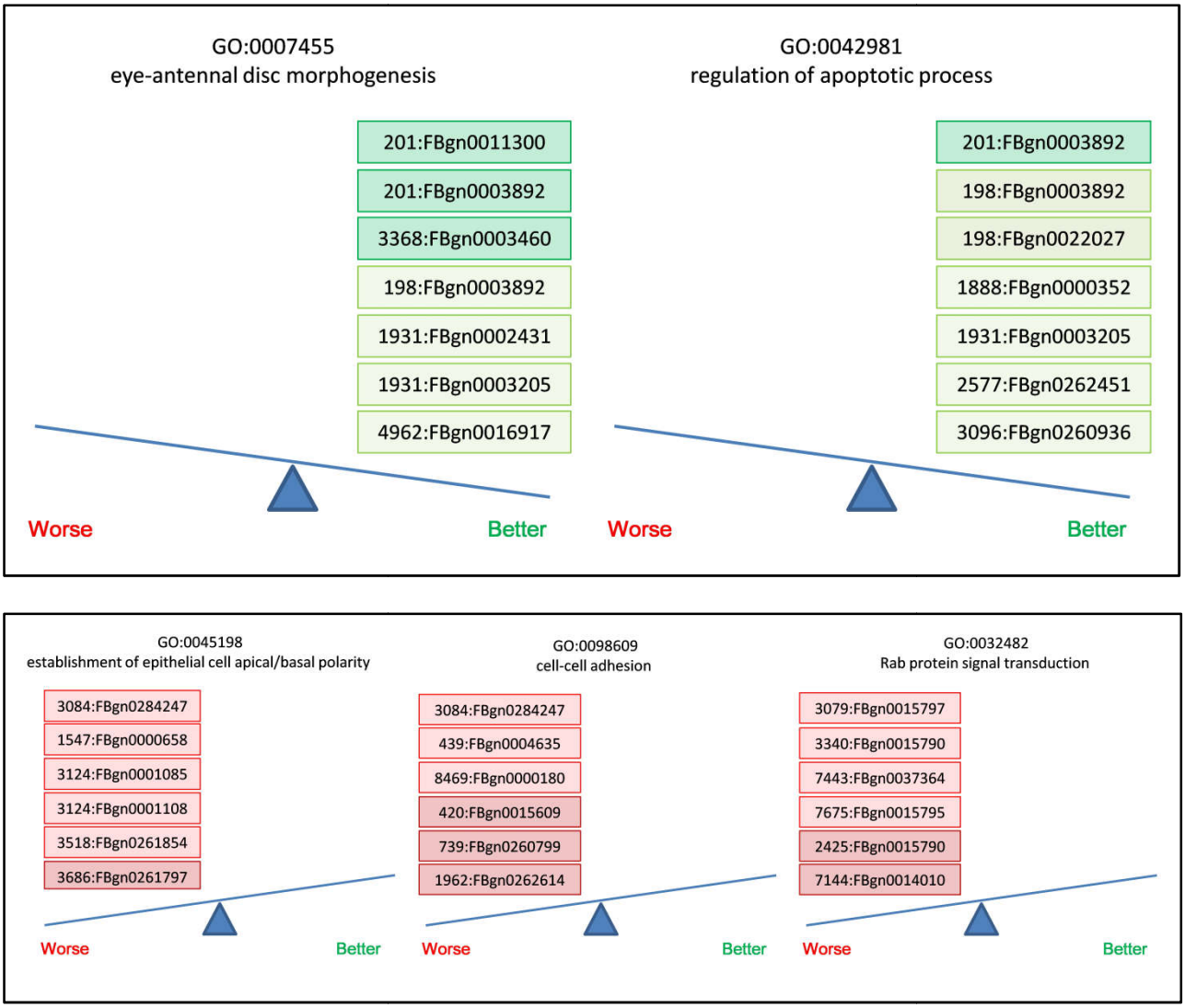

Figure 22. Schematic representation of the top GO results for ameliorative and pejorative phenotypes. The GO classes with better stock/genes frequency for the ameliorative (upper panel) and pejorative (lower panel) phenotype. Every rectangle represent a single annotated gene (FBgn#), and the other number present is the BDSC stock#. Rectangles colors represent phenotypic classes class -1 (light red), class -2 (dark red), class +1 (light green) and class +2 (dark green).

GO BIOLOGICAL PROCESS #	GO worse	GO better	Sum	GO description	Total Frequency	FlyBase gene annotation (FBgn)	Stock #	Phenotype
GO:0007455	0	7	13,02928302	eye-antennal disc morphogenesis	7	FBgn0011300 FBgn0003892 FBgn0003460 FBgn0003892 FBgn0002431 FBgn0003205 FBgn0016917	201 201 3368 198 1931 1931 4962	2 2 2 1 1 1 1
GO:0042981	0	7	13,02928302	regulation of apoptotic process	7	FBgn0003892 FBgn0003892 FBgn0022027 FBgn0000352 FBgn0003205 FBgn0262451 FBgn0260936	201 198 198 1888 1931 2577 3096	2 1 1 1 1 1 1
GO:0045198	6	0	11,8068906	establishment of epithelial cell apical/basal polarity	6	FBgn0000658 FBgn0284247 FBgn0001085 FBgn0001108 FBgn0261854 FBgn0261797	1547 3084 3124 3124 3518 3686	-1 -1 -1 -1 -1 -2
GO:0098609	6	0	11,8068906	cell-cell adhesion	6	FBgn0004635 FBgn0284247 FBgn0000180 FBgn0015609 FBgn0260799 FBgn0262614	439 3084 8469 420 739 1962	-1 -1 -1 -2 -2 -2
GO:0032482	6	0	11,8068906	Rab protein signal transduction	6	FBgn0015797 FBgn0015790 FBgn0037364 FBgn0015795 FBgn0015790 FBgn0014010	3079 3340 7443 7675 2425 7144	-1 -1 -1 -1 -2 -2

Table 3. Extract of GO results for top ameliorative and pejorative phenotypes.

4.8 Rab genes as a new potential family involved in pathological BCR-ABL1 mechanism

With respect to all GO observed in Figure 22, that involved large genes families ("regulation of apoptotic process" and "cell-cell adhesion"), the GO:0032482 class stand out for gene pathways specificity: "Rab protein signal transduction". The genes identified in this family include: FBgn0015797 (Rab6), FBgn0014010 (Rab5), FBgn0015795 (Rab7), FBgn0037364 (Rab23) and

FBgn0015790 (Rab11), the only one found in two independent stocks. Intriguingly, with respect to all of the other stocks in this family that affect several genes, only three genes were completely destroyed in the stock #7144: Rab5, eys, and Sec24CD. Furthermore, F1 generation obtained between #7144 stock and *gmrGal4,UAS-BCR-ABL1 4M/TM3* showed a particularly severe worsening of the BCR-ABL1 phenotype (Figure 23 and 24, left red block). Since the deficiency stock of *Rab5* involved other two genes, we decided to validate the phenotype observed in #7144 and see if the modulation of *Rab5* alone would have shown the same changes in the BCR-ABL1 induced phenotype. We crossed the BCR-ABL1 transgenic flies with 3 different stocks of *Drosophila* bearing different mutated *Rab5*. In detail, we used one stock of *Rab5* expressing a dominant-negative isoform of the protein (*Rab5.S43N DN*), one overexpressing the wild type isoform (*UAS Rab5 wt*) and one encoding a constitutively active isoform (*UAS Rab5.Q88L*). The eyes of the flies co-expressing BCR-ABL1 and the dominant-negative (DN) of *Rab5* showed a marked worsening of the BCR-ABL1 phenotype, affecting the normal round morphology and pigmentation, and showing areas of necrosis (Figure 24, right red block). Furthermore, the co-expression of BCR-ABL1 and the overexpression of either the wild type allele or the constitutively active isoform of *Rab5* partially rescued the BCR-ABL1 phenotype (Figure 24, green panels).

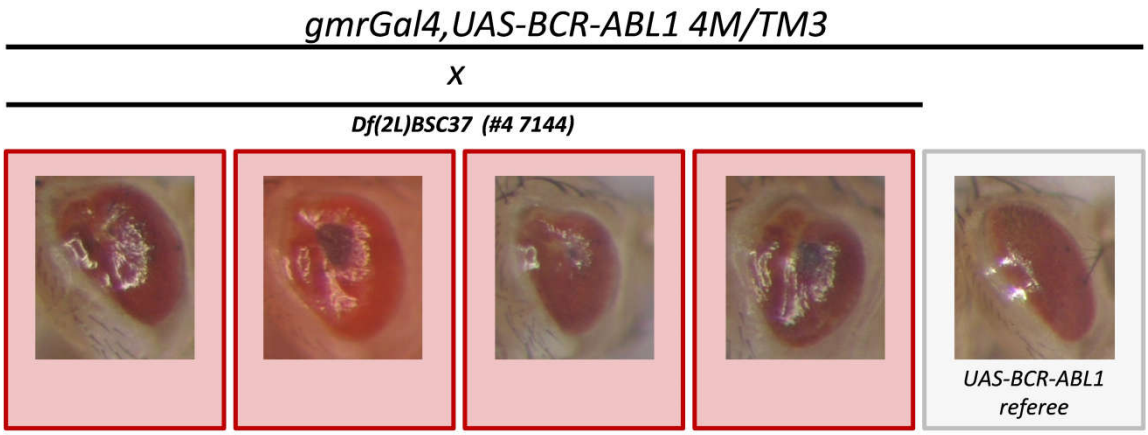

Figure 23. F1 generation obtained by crossing #7144 stock and *gmrGal4,UAS-BCR-ABL1 4M/TM3.* BCR-ABL1 induced phenotype is strongly worsened by crossing with deficiency *Df(2L)BSC37 (#4 7144)*, a deletion that contains three genes only, among which is Rab5.

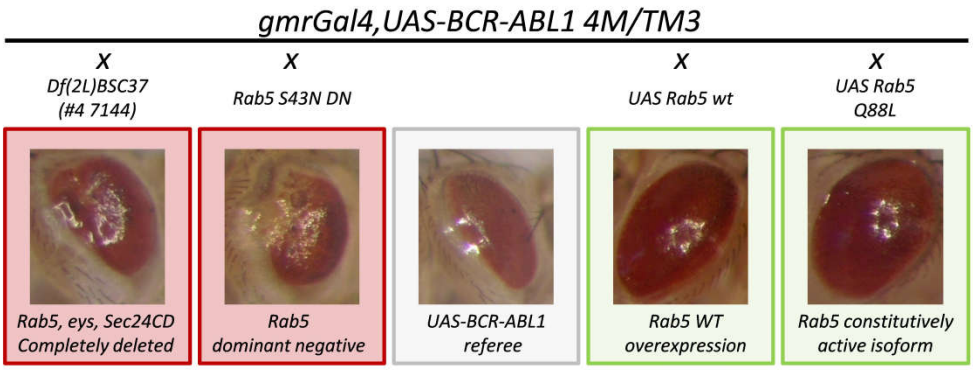

Figure 24. Phenotypes modifications involving Rab5. In detail, from left to right: *Df(2L)BSC37(#4 7144*) and stock expressing a dominant negative isoform of Rab5 (*Rab5.S43N DN*), showing strong worsening of the phenotype (red panels); *gmrGal4,UAS-BCR-ABL1 4M/TM3* phenotype referee (grey panel); stock overexpressing the wild type Rab5 (*UAS Rab5 wt*) and stock encoding a constitutively active isoform of Rab5 (*UAS Rab5.Q88L*), showing a clear improvement of the phenotype (green panels).

Supported by the promising data obtained by our screening, we decided to evaluate mRNA expression levels of *RAB5A*, the principal human ortholog of *Drosophila Rab5*, in healthy controls and CML patients. To perform this, we collected several PB and BM patients' specimens at different stages of the disease: at diagnosis (Diagnosis), during at least cytogenetic remission (Remission), and during secondary resistance (Relapse). In addition, other 10 specimens were collected by patients during primary resistance to TKI (Resistant). Interestingly, the qRT-PCR analysis revealed a significant downregulation of *RAB5A* in CML patients at diagnosis (mean -0.98; CI 1.34–2.69; T-test p<<0.01), after relapse (mean -0.97; CI 1.25–2.77; T-test p<<0.01), and in resistant subjects (mean -2.46; CI 0.53–6.46; T-test p=0.02) compared to healthy controls (mean +1.04) (Figure 25A upper panel). In contrast, when we observed clinical disease remission the expression of *RAB5A* increased, achieving the same levels observed in healthy donors (mean +0.78; CI -0.43–0.95; T-test p=0.44). This pattern was also observed when we stratified specimens by sample types (BM or PB) (Figure 26). Our data suggest an inverse correlation between *RAB5A* expression and the presence of *BCR-ABL1* transcript, highlighted by their opposite behavior (Figure 25A). To investigate this association we dichotomized *RAB5A* expression and we evaluated correlation with *BCR-ABL1* transcript, subdivided using two clinical diagnostic *BCR-ABL1* levels thresholds: cytogenetic (<1%) and molecular remission (<0.1%). We observed significant opposite regulation of these two

transcripts (Figure 25B), suggesting a direct downmodulation of *RAB5A* in the presence of the Philadelphia chromosome (cytological: p<<0.01; odds ratio 0.05; CI 0.01–0.15; molecular: p<<0.01; odds ratio 0.06; CI 0.01–0.21). This data is consistent with what we observed in *Drosophila*, meaning *RAB5A* could potentially be a new target gene involved in BCR-ABL1 pathological signaling.

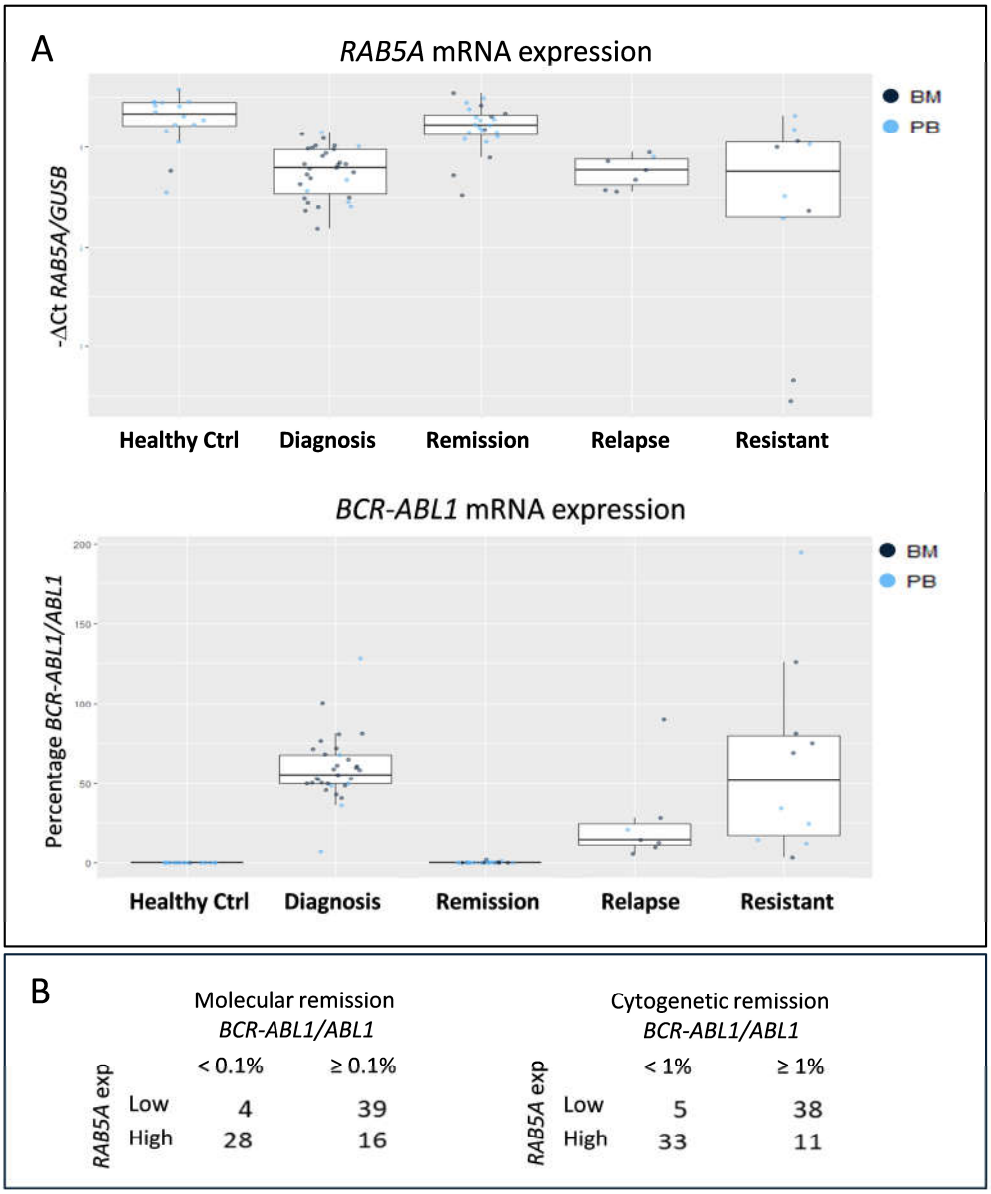

Figure 25. Significant downregulation of *RAB5A* mRNA expression in CML patients. (A) Modulations of *RAB5A and BCR-ABL1* were analyzed with *t* test in CML patients at different stages of disease and in healthy controls. BM, bone marrow; PB, peripheral blood **(B)** Relationships between *RAB5A* expression levels and *BCR-ABL1/ABL1* percentage. *RAB5A* was dichotomized basing on median value, while *BCR-ABL1/ABL1* was stratified by molecular (left panel) and cytogenetic (right panel) remission.

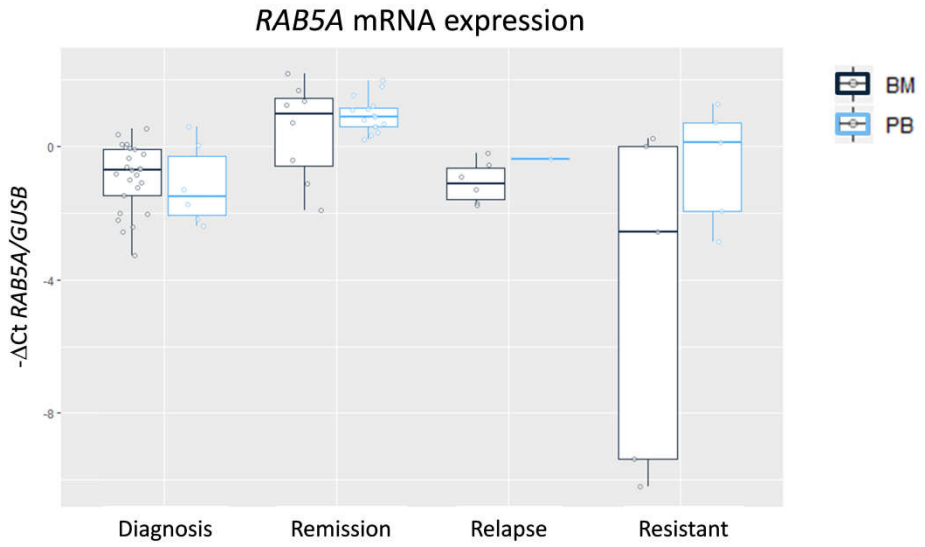

Figure 26. RAB5A mRNA expression levels in CML patients subdivided in bone marrow o peripheral blood samples show the same pattern.

5. DISCUSSION

In order to identify candidate genes and pathways involved in CML onset and progression we developed and validated a CML genetic model based on transgenic *Drosophila* expressing BCR-ABL1. To build and characterize a human functional model that could be sensitive to pharmacological inhibition and suitable to study the effect of the BCR-ABL1 mutations identified in leukemia patients, we chose to express a completely human p210-BCR-ABL1 protein, differently from what has been previously done[55]. The expression of the oncoprotein in all eye cells committed to differentiation as photoreceptors or accessory cells (*gmrGal4* driver) induces a strong phenotype characterized by altered differentiation of the ommatidia cells[92]. The lack of phenotype in flies expressing the BCR-ABL1 kinase-dead mutant supports the role of the kinase activity on the eye phenotype. Moreover, BCR-ABL1 expression and phosphorylation levels correlates with the severity of the phenotype. Consistently, BCR-ABL1 expression under the control of *gmrGal4* induces decrease of photoreceptors expressing Elav in eye imaginal discs and this correlates with the disruption of the adult eye. Interestingly, partial loss of *dAbl* function as well mildly reduces the number of eye cells expressing Elav at L3, and much more severely at later stages of development. This suggests that *dAbl* is implicated in maintenance of the neuronal commitment[93,94] and confirms that loss or gain of function of dAbl/BCR-ABL1 can alter eye cell development[55]. We have shown that human BCR-ABL1 interacts and interferes with the dAbl signaling pathway. Animals expressing BCR-ABL1 and heterozygous for the recessive Abl^{1} allele or coexpressing either *Abl-RNAi* or a kinase-dead dominant negative *Abl* (Abl^{K417N}) showed a weaker phenotype, suggesting that BCR-ABL1 and dAbl proteins most likely share binding sites and/or targets of the kinase activity. Consistently, coexpression of human BCR-ABL1 and dAbl synergizes and the phenotype becomes more severe. Notably, dAbl overexpression *per se* induces a weak “rough” eye phenotype but the differentiation program is not severely disrupted. We cannot exclude that this is due to a level of dAbl expression below a critic threshold but it could also suggests that excessive dAbl might be still, at least partially, negatively regulated. This possible negative regulation seems

to be overcome by BCR-ABL1 since all animals coexpressing dAbl and BCR-ABL1 showed a severe class -1 phenotype. Consistently, LOF or downregulation of genes known to genetically interact with *dAbl* LOF mutations interact in the same way with BCR-ABL1 expression. Namely, *pros* and *fax* alleles or deletions enhance the phenotype and this is consistent with their roles in neuronogenesis and neuronal differentiation. Moreover, either *ena* or *Dab* LOF, respectively, suppresses or enhances the *dAbl* LOF phenotype[67,68] and we observed that both *ena* or *Dab* LOF and downregulation through RNAi modify in the same way also the BCR-ABL1 phenotype. Ena belongs to the ENA/VASP protein family involved in regulation of the actin cytoskeleton[95,96]. dAbl regulates Ena by modulating its localization most likely through its phosphorylation. It is known that both dAbl and the human/*Drosophila* BCR-ABL chimera phosphorylate Ena[55] in vitro and we established that also human BCR-ABL1 expression in the eye increases Ena phosphorylation. This conservation of phosphorylation targets significantly increases the reliability of our model to identify relevant BCR-ABL1 functional interactors. In this view the observation that decreased Ena function suppresses phenotypes due to both *dAbl* mutations[73] and BCR-ABL1 expression suggests that both phenotypes can be due to Ena mislocalization and consequently actin cytoskeleton alterations that can be suppressed if Ena expression decreases. In *Drosophila, Abl* and *Dab* are often coexpressed and the phenotype due to *Dab* mutations mimics *dAbl* phenotype. Epistasis experiments have shown that *Dab* functions upstream of both dAbl and Ena, controlling their localization and thus the actin cytoskeleton, and *Dab* LOF indeed enhances the phenotype due to *dAbl* mutations[79]. Interestingly, *Dab* deletion or downregulation has the same effect on the BCR-ABL1 phenotype. This evidence might be explained if Dab is able to regulate, at least partially, BCR-ABL1 localization. This interaction might mitigate more severe BCR-ABL1 dependent effects when *Dab* is expressed at physiological level but not if *Dab* is downregulated or its gene dosage is halved. Furthermore, our study showed that Dab human homologs are less expressed both in PB and BM of CML patients at diagnosis compared to controls and are re-expressed in patients during MR. Moreover, Dab1 expression in transfected K562 cells significantly

decreases cell proliferation confirming that Dab activity might alleviate BCR-ABL1 pathogenic effects. Then, we assessed if our model could likely lead to fish-out homologs of leukemia relevant genes in an ongoing dosage sensitive genetic screen challenging the whole *Drosophila* genome. To this aim we considered STAT5, a transcription factor phosphorylated and activated by BCR-ABL1. Interestingly, LOF conditions of *STAT92E*, encoding the fly homolog of human STATs, led to suppression of the BCR-ABL1 phenotype. To find out a tissue that could be a reliable second read-out to identify BCR-ABL1 interactors relevant for hematopoiesis and leukemia, we moved to the larval hematopoietic organ, the lymph gland. We conditionally expressed human BCR-ABL1 in the lymph gland medullary zone (MZ) where quiescent prohemocytes reside. Only BCR-ABL1 expression during L2 induces the appearance of melanotic nodules that correlates with the increase of circulating hemocytes and this phenotype can be suppressed by *dAbl* downregulation. This confirms that *dAbl* is expressed in the lymph gland MZ[91] where it contributes to BCR-ABL1 pathway activation and to the induction of the hematopoietic phenotype. Noteworthy, both *Dab* and *ena* functionally interact with BCR-ABL1 during hematopoiesis. In fact, while *Dab* downregulation enhances the melanotic nodules phenotype and Dab overexpression suppresses it, *ena* downregulation decreases the penetrance of this phenotype, confirming that also in the lymph gland MZ *ena* and *Dab* are expressed[91] and modulate BCR-ABL1 activity. This phenotype is visible if BCR-ABL1 is expressed from the L2, when prohemocytes become quiescent, but not if it is expressed from the early L3, when the quiescent prohemocytes are still present in the MZ of the lymph gland. We are tempted to speculate that the dAbl pathway, activated by BCR-ABL1, could be involved in the mechanisms that regulate the prohemocytes entrance into the quiescence state rather than its maintenance. This seems consistent with the observation that in mid-L3 larvae expressing BCR-ABL1 from L2, the lymph glands are very small compared to controls and do not show any clear partition. This suggests that, upon BCR-ABL1 expression, most of the prohemocytes could undertake the differentiation pathway and leave the lymph gland prematurely without becoming quiescent. We did not test all pathways interacting with BCR-ABL1, for example

the Tyr-receptor/Ras pathway known to compete with BCR-ABL1 for binding with the Grb2/Drk proteins[1] and that is likely involved in the eye phenotype since the Sevenless Tyr-receptor has an established role in eye differentiation[50,97]. Nevertheless, we presented a new and efficient CML model based on transgenic *Drosophila* for human BCR-ABL1 that is a powerful tool to identify new genes and pathways involved in the pathogenesis and progression of CML. To do so we conducted a genome-wide genetic screening using commercial genes deletion stocks for autosomal chromosomes 2 and 3 and our previously generated and validated CML *Drosophila* model, *gmrGal4,UAS-BCR-ABL1 4M/TM3*, as 'bait'[56].

Although deletion stocks include several genes often partially or completely destroyed generating complex phenotypes, we were able to filter out some important information that could enrich the knowledge of the BCR-ABL1 pathological pathway. In particular, we identified two GO families concerning ameliorative phenotype: "regulation of apoptotic process" and "cell-cell adhesion". As members of these two classes, we identified *patched* gene (FBgn0003892), an ortholog to human *PTCH1* (*patched 1*) and *PTCH2* (*patched 2*). Protein patched homolog 1 (PTCH1) encodes for a cell-surface receptor and is a member of the Hedgehog (Hh) signaling pathway. The PTCH1 protein exerts its function by negatively regulating the activity of the frizzled family receptor smoothened (SMO)[98]. There is evidence that this pathway plays a critical role in the etiopathogenesis of various hemopoietic malignancies, in particular in CML[99]. It has been reported in the literature that Hh signaling is increased in BCR-ABL1 progenitor cells and it is further upregulated during disease progression[100]. Furthermore, *PTCH1* overexpression and mutations in CML patients are associated with poor prognosis, relapse or resistance to TKIs[101-104]. All this data supports our analysis, where the suppression of the *patched* gene generates a better phenotype, suggesting that BCR-ABL1 and patched, when present together, cooperate to the disease etiopathogenesis. In addition, among genes of "eye-antennal disc morphogenesis", we found *babo* (FBgn0011300), a gene activated by patched and SMO signaling in *Drosophila*[105]. Intriguingly, *babo* is ortholog of *TGFBR1* (best score), a representative of Transforming Growth Factor-β Receptor family (TGF-

βR). It is known that the TGF-βR signaling pathway plays an important role in CML, leading to cell growth inhibition, differentiation, and apoptosis[106]. Interestingly, when *patched* and *babo* were simultaneously deleted, as in stock #201, we observe better phenotype respect to #198, where only *patched* is suppressed. This result could indicate, also in this case, the powerful cooperation of these genes with the BCR-ABL1 pathway, highlighting how *Drosophila* can be considered a powerful model system to identify positive and negative interactors of BCR-ABL1.

We identified some genes that could cooperate with BCR-ABL1 in CML also in the worse phenotype classes. One of these is *frizzled* (FBgn0001085), a seven-pass transmembrane domain receptor, ortholog of human *FZD7*, a gene involved in CML cells protection mediated by bone marrow-derived mesenchymal stem cells[107]. Recent evidence suggests that atypical G protein-coupled receptors (GPCRs) Frizzled and SMO also regulate the Hippo pathway in a G protein-dependent manner and contribute to the crosstalk between Hippo and other important pathways (such as Wnt and Hh) in development and cancer[108]. BCR-ABL1 involvement in these fundamental biological processes was also supported by our screening, in which we identified several other genes participating in these pathways, such as *aPKC* (FBgn0261854) and *four-jointed* (FBgn0000658). Furthermore, interactions with cadherins molecular pathway (dachsous [FBgn0284247], Cadherin-N[FBgn0015609], and Adherens junction protein p120 [FBgn0260799]) were also identified and supported by literature data. Indeed, Zang et al. reported that N-cadherin expression contributes to increased resistance to farnesyltransferase inhibitor SCH66336 in BCR-ABL1-P190 lymphoblastic leukemia cells[109]. Furthermore, Mu et al. identified that the expression of *CDH13n*mRNA in CML patients was lower than in the healthy adults, showing a negative correlation with the *BCR-ABL1* fusion gene, that may contribute in CML development[110].

In our analysis, we also identified for the first time a tight interconnection between BCR-ABL1 expression and Rab family (Rab5 [FBgn0014010], Rab6 [FBgn0015797], Rab7 [FBgn0015795], Rab11 [FBgn0015790], Rab23 [FBgn0037364]) proteins and microtubule-based kinesin and cytoplasmic dynein motor complexes, that are the prominent class of Rab effectors (Dhc64C

[FBgn0261797], DCTN1-p150 [FBgn0001108]). The Rab GTPase proteins were first studied in yeast *S. cerevisiae* and are the master regulators of all stages of intracellular trafficking processes in eukaryotic cells, evolutionarily conserved from fly to vertebrates. *RAB5* gene, which encodes for a monomeric small GTPase, is a key member of the Rab family, and *RAB5A* is its most important subtype, with well-identified functions and mechanisms. RAB5A affects the internalization and intracellular transport of receptors, such as receptor tyrosine kinases, GPCRs, and antigen recognition receptors by recruiting Rab5 effectors. The signals mediated by RAB5A range between gene transcription, cell morphology, growth, differentiation, apoptosis, and disease development[111]. In our analysis, we observed a worsening of the BCR-ABL1-induced phenotype in the absence of Rab5 expression and this data were concordant with results obtained with other members of the Rab family, identified in our screening. This scenario was also confirmed in CML patients' specimens, where the expression of *RAB5A* transcript was significantly reduced in pathological state, while returned to normal levels during the remission phase. In addition, we identified a significant opposite regulation of *BCR-ABL1* and *RAB5A* mRNA. *BCR-ABL1* transcript, when present, would seem to downmodulate *RAB5A* expression, probably in order to acquire some molecular advantages, as reducing receptor turnover and increasing proliferative stimuli. In support of this hypothesis, we previously identified that downregulation of Rab interactor 1 (RIN1) and Bridging integrator 1 (BIN1), two proteins directly involved with Rab-mediated receptor tyrosine kinase intracellular trafficking, caused an aberrant and constitutive receptor signaling and are often observed deregulated in CML resistant patients[112].

6. CONCLUSIONS

In conclusion, we presented a new and efficient CML model based on transgenic *Drosophila* for human BCR-ABL1 and we conducted a genetic screening searching for new interactors. Our data suggest that BCR-ABL1 regulates several important biological pathways that could affect CML subtypes, such as Rab family proteins. The knowledge of these biological ways could be useful in the future to better discriminate CML patients and to develop new potential therapeutic targets for the treatment of CML-resistant patients. Although some other studies will be needed to validate all putative BCR-ABL1 interactors identified in this work, the *Drosophila* appeared to be a powerful tool to dissect BCR-ABL1 etiopathological mechanisms.

7. REFERENCES

1. Chereda, B.; Melo, J.V. Natural course and biology of CML. *Annals of hematology* **2015**, *94 Suppl 2*, S107-121, doi:10.1007/s00277-015-2325-z.

2. Quintas-Cardama, A.; Cortes, J. Molecular biology of bcr-abl1-positive chronic myeloid leukemia. *Blood* **2009**, *113*, 1619-1630, doi:10.1182/blood-2008-03-144790.

3. Baccarani, M.; Saglio, G.; Goldman, J.; Hochhaus, A.; Simonsson, B.; Appelbaum, F.; Apperley, J.; Cervantes, F.; Cortes, J.; Deininger, M., et al. Evolving concepts in the management of chronic myeloid leukemia: recommendations from an expert panel on behalf of the European LeukemiaNet. *Blood* **2006**, *108*, 1809-1820, doi:10.1182/blood-2006-02-005686.

4. Benson, E.S. Leukemia and the Philadelphia chromosome. *Postgraduate medicine* **1961**, *30*, A22-A28.

5. Groffen, J.; Stephenson, J.R.; Heisterkamp, N.; de Klein, A.; Bartram, C.R.; Grosveld, G. Philadelphia chromosomal breakpoints are clustered within a limited region, bcr, on chromosome 22. *Cell* **1984**, *36*, 93-99, doi:10.1016/0092-8674(84)90077-1.

6. Groffen, J.; Stephenson, J.R.; Heisterkamp, N.; Bartram, C.; de Klein, A.; Grosveld, G. The human c-abl oncogene in the Philadelphia translocation. *Journal of cellular physiology. Supplement* **1984**, *3*, 179-191, doi:10.1002/jcp.1041210421.

7. Zhou, T.; Medeiros, L.J.; Hu, S. Chronic Myeloid Leukemia: Beyond BCR-ABL1. *Current hematologic malignancy reports* **2018**, *13*, 435-445, doi:10.1007/s11899-018-0474-6.

8. Shuai, K.; Halpern, J.; ten Hoeve, J.; Rao, X.; Sawyers, C.L. Constitutive activation of STAT5 by the BCR-ABL oncogene in chronic myelogenous leukemia. *Oncogene* **1996**, *13*, 247-254.

9. Jain, S.K.; Susa, M.; Keeler, M.L.; Carlesso, N.; Druker, B.; Varticovski, L. PI 3-kinase activation in BCR/abl-transformed hematopoietic cells does not require interaction of p85 SH2 domains with p210 BCR/abl. *Blood* **1996**, *88*, 1542-1550.

10. Varticovski, L.; Daley, G.Q.; Jackson, P.; Baltimore, D.; Cantley, L.C. Activation of phosphatidylinositol 3-kinase in cells expressing abl oncogene variants. *Molecular and cellular biology* **1991**, *11*, 1107-1113, doi:10.1128/mcb.11.2.1107.

11. Birge, R.B.; Kalodimos, C.; Inagaki, F.; Tanaka, S. Crk and CrkL adaptor proteins: networks for physiological and pathological signaling. *Cell communication and signaling : CCS* **2009**, *7*, 13, doi:10.1186/1478-811X-7-13.

12. Wee, P.; Wang, Z. Epidermal Growth Factor Receptor Cell Proliferation Signaling Pathways. *Cancers* **2017**, *9*, doi:10.3390/cancers9050052.

13. Ilaria, R.L., Jr.; Van Etten, R.A. P210 and P190(BCR/ABL) induce the tyrosine phosphorylation and DNA binding activity of multiple specific STAT family members. *The Journal of biological chemistry* **1996**, *271*, 31704-31710.

14. Nowicki, M.O.; Falinski, R.; Koptyra, M.; Slupianek, A.; Stoklosa, T.; Gloc, E.; Nieborowska-Skorska, M.; Blasiak, J.; Skorski, T. BCR/ABL oncogenic kinase promotes unfaithful repair of the reactive oxygen species-dependent DNA double-strand breaks. *Blood* **2004**, *104*, 3746-3753, doi:10.1182/blood-2004-05-1941.

15. Hoover, R.R.; Gerlach, M.J.; Koh, E.Y.; Daley, G.Q. Cooperative and redundant effects of STAT5 and Ras signaling in BCR/ABL transformed hematopoietic cells. *Oncogene* **2001**, *20*, 5826-5835, doi:10.1038/sj.onc.1204549.

16. Gaymes, T.J.; Mufti, G.J.; Rassool, F.V. Myeloid leukemias have increased activity of the nonhomologous end-joining pathway and concomitant DNA misrepair that is dependent on the Ku70/86 heterodimer. *Cancer research* **2002**, *62*, 2791-2797.

17. Albajar, M.; Gomez-Casares, M.T.; Llorca, J.; Mauleon, I.; Vaque, J.P.; Acosta, J.C.; Bermudez, A.; Donato, N.; Delgado, M.D.; Leon, J. MYC in chronic myeloid leukemia: induction of aberrant DNA synthesis and association with poor response to imatinib. *Molecular cancer research : MCR* **2011**, *9*, 564-576, doi:10.1158/1541-7786.MCR-10-0356.

18. Mu, Q.; Ma, Q.; Wang, Y.; Chen, Z.; Tong, X.; Chen, F.F.; Lu, Y.; Jin, J. Cytogenetic profile of 1,863 Ph/BCR-ABL-positive chronic myelogenous leukemia patients from the Chinese population. *Annals of hematology* **2012**, *91*, 1065-1072, doi:10.1007/s00277-012-1421-6.

19. Johansson, B.; Fioretos, T.; Mitelman, F. Cytogenetic and molecular genetic evolution of chronic myeloid leukemia. *Acta haematologica* **2002**, *107*, 76-94, doi:10.1159/000046636.

20. Calabretta, B.; Perrotti, D. The biology of CML blast crisis. *Blood* **2004**, *103*, 4010-4022, doi:10.1182/blood-2003-12-4111.

21. Faderl, S.; Kantarjian, H.M.; Talpaz, M. Chronic myelogenous leukemia: update on biology and treatment. *Oncology* **1999**, *13*, 169-180; discussion 181, 184.

22. Deininger, M.W.; Goldman, J.M.; Melo, J.V. The molecular biology of chronic myeloid leukemia. *Blood* **2000**, *96*, 3343-3356.

23. Hoglund, M.; Sandin, F.; Simonsson, B. Epidemiology of chronic myeloid leukaemia: an update. *Annals of hematology* **2015**, *94 Suppl 2*, S241-247, doi:10.1007/s00277-015-2314-2.

24. Hochhaus, A.; Baccarani, M.; Silver, R.T.; Schiffer, C.; Apperley, J.F.; Cervantes, F.; Clark, R.E.; Cortes, J.E.; Deininger, M.W.; Guilhot, F., et al. European LeukemiaNet 2020 recommendations for treating chronic myeloid leukemia. *Leukemia* **2020**, *34*, 966-984, doi:10.1038/s41375-020-0776-2.

25. Heyssel, R.; Brill, A.B.; Woodbury, L.A.; Nishimura, E.T.; Ghose, T.; Hoshino, T.; Yamasaki, M. Leukemia in Hiroshima atomic bomb survivors. *Blood* **1960**, *15*, 313-331.

26. Baccarani, M.; Deininger, M.W.; Rosti, G.; Hochhaus, A.; Soverini, S.; Apperley, J.F.; Cervantes, F.; Clark, R.E.; Cortes, J.E.; Guilhot, F., et al. European LeukemiaNet recommendations for the management of chronic myeloid leukemia: 2013. *Blood* **2013**, *122*, 872-884, doi:10.1182/blood-2013-05-501569.

27. Baccarani, M.; Cortes, J.; Pane, F.; Niederwieser, D.; Saglio, G.; Apperley, J.; Cervantes, F.; Deininger, M.; Gratwohl, A.; Guilhot, F., et al. Chronic myeloid leukemia: an update of concepts and management recommendations of European LeukemiaNet. *Journal of clinical oncology : official journal of the American Society of Clinical Oncology* **2009**, *27*, 6041-6051, doi:10.1200/JCO.2009.25.0779.

28. Sokal, J.E.; Cox, E.B.; Baccarani, M.; Tura, S.; Gomez, G.A.; Robertson, J.E.; Tso, C.Y.; Braun, T.J.; Clarkson, B.D.; Cervantes, F., et al. Prognostic discrimination in "good-risk" chronic granulocytic leukemia. *Blood* **1984**, *63*, 789-799.

29. Geelen, I.G.P.; Sandin, F.; Thielen, N.; Janssen, J.; Hoogendoorn, M.; Visser, O.; Cornelissen, J.J.; Hoglund, M.; Westerweel, P.E. Validation of the EUTOS long-term survival score in a recent independent cohort of "real world" CML patients. *Leukemia* **2018**, *32*, 2299-2303, doi:10.1038/s41375-018-0136-7.

30. Pfirrmann, M.; Baccarani, M.; Saussele, S.; Guilhot, J.; Cervantes, F.; Ossenkoppele, G.; Hoffmann, V.S.; Castagnetti, F.; Hasford, J.; Hehlmann, R., et al. Prognosis of long-term survival considering disease-specific death in patients with chronic myeloid leukemia. *Leukemia* **2016**, *30*, 48-56, doi:10.1038/leu.2015.261.

31. Lauseker, M.; Hanfstein, B.; Haferlach, C.; Schnittger, S.; Pfirrmann, M.; Fabarius, A.; Schlegelberger, B.; Saussele, S.; Dietz, C.T.; Erben, P., et al. Equivalence of BCR-ABL transcript levels with complete cytogenetic remission in patients with chronic myeloid leukemia in chronic phase. *Journal of cancer research and clinical oncology* **2014**, *140*, 1965-1969, doi:10.1007/s00432-014-1746-8.

32. Cross, N.C.; White, H.E.; Colomer, D.; Ehrencrona, H.; Foroni, L.; Gottardi, E.; Lange, T.; Lion, T.; Machova Polakova, K.; Dulucq, S., et al. Laboratory recommendations for scoring deep molecular responses following treatment for chronic myeloid leukemia. *Leukemia* **2015**, *29*, 999-1003, doi:10.1038/leu.2015.29.

33. Goldman, J.M.; Marin, D.; Olavarria, E.; Apperley, J.F. Clinical decisions for chronic myeloid leukemia in the imatinib era. *Seminars in hematology* **2003**, *40*, 98-103; discussion 104-113, doi:10.1053/shem.2003.50049.

34. O'Brien, S.G.; Guilhot, F.; Larson, R.A.; Gathmann, I.; Baccarani, M.; Cervantes, F.; Cornelissen, J.J.; Fischer, T.; Hochhaus, A.; Hughes, T., et al. Imatinib compared with interferon and low-dose cytarabine for newly diagnosed chronic-phase chronic myeloid leukemia. *The New England journal of medicine* **2003**, *348*, 994-1004, doi:10.1056/NEJMoa022457.

35. Druker, B.J.; Tamura, S.; Buchdunger, E.; Ohno, S.; Segal, G.M.; Fanning, S.; Zimmermann, J.; Lydon, N.B. Effects of a selective inhibitor of the Abl tyrosine kinase on the growth of Bcr-Abl positive cells. *Nature medicine* **1996**, *2*, 561-566, doi:10.1038/nm0596-561.

36. Druker, B.J.; Guilhot, F.; O'Brien, S.G.; Gathmann, I.; Kantarjian, H.; Gattermann, N.; Deininger, M.W.; Silver, R.T.; Goldman, J.M.; Stone, R.M., et al. Five-year follow-up of patients receiving imatinib for chronic myeloid leukemia. *The New England journal of medicine* **2006**, *355*, 2408-2417, doi:10.1056/NEJMoa062867.

37. Braun, T.P.; Eide, C.A.; Druker, B.J. Response and Resistance to BCR-ABL1-Targeted Therapies. *Cancer cell* **2020**, *37*, 530-542, doi:10.1016/j.ccell.2020.03.006.

38. Nardi, V.; Azam, M.; Daley, G.Q. Mechanisms and implications of imatinib resistance mutations in BCR-ABL. *Current opinion in hematology* **2004**, *11*, 35-43, doi:10.1097/00062752-200401000-00006.

39. Talpaz, M.; Shah, N.P.; Kantarjian, H.; Donato, N.; Nicoll, J.; Paquette, R.; Cortes, J.; O'Brien, S.; Nicaise, C.; Bleickardt, E., et al. Dasatinib in imatinib-resistant Philadelphia chromosome-positive leukemias. *The New England journal of medicine* **2006**, *354*, 2531-2541, doi:10.1056/NEJMoa055229.

40. Soverini, S.; Bavaro, L.; De Benedittis, C.; Martelli, M.; Iurlo, A.; Orofino, N.; Sica, S.; Sora, F.; Lunghi, F.; Ciceri, F., et al. Prospective assessment of NGS-detectable mutations in CML patients with nonoptimal response: the NEXT-in-CML study. *Blood* **2020**, *135*, 534-541, doi:10.1182/blood.2019002969.

41. Soverini, S.; Abruzzese, E.; Bocchia, M.; Bonifacio, M.; Galimberti, S.; Gozzini, A.; Iurlo, A.; Luciano, L.; Pregno, P.; Rosti, G., et al. Next-generation sequencing for BCR-ABL1 kinase domain mutation testing in patients with chronic myeloid leukemia: a position paper. *Journal of hematology & oncology* **2019**, *12*, 131, doi:10.1186/s13045-019-0815-5.

42. Myers, E.W.; Sutton, G.G.; Delcher, A.L.; Dew, I.M.; Fasulo, D.P.; Flanigan, M.J.; Kravitz, S.A.; Mobarry, C.M.; Reinert, K.H.; Remington, K.A., et al. A whole-genome assembly of Drosophila. *Science* **2000**, *287*, 2196-2204, doi:10.1126/science.287.5461.2196.

43. Paulson, R.; Jackson, J.; Immergluck, K.; Bishop, J.M. The DFer gene of Drosophila melanogaster encodes two membrane-associated proteins that can both transform vertebrate cells. *Oncogene* **1997**, *14*, 641-652, doi:10.1038/sj.onc.1200875.

44. Schejter, E.D.; Shilo, B.Z. Characterization of functional domains of p21 ras by use of chimeric genes. *The EMBO journal* **1985**, *4*, 407-412.

45. Klueg, K.M.; Alvarado, D.; Muskavitch, M.A.; Duffy, J.B. Creation of a GAL4/UAS-coupled inducible gene expression system for use in Drosophila cultured cell lines. *Genesis* **2002**, *34*, 119-122, doi:10.1002/gene.10148.

46. Duffy, J.B. GAL4 system in Drosophila: a fly geneticist's Swiss army knife. *Genesis* **2002**, *34*, 1-15, doi:10.1002/gene.10150.

47. Brand, A.H.; Perrimon, N. Targeted gene expression as a means of altering cell fates and generating dominant phenotypes. *Development* **1993**, *118*, 401-415.

48. Stilwell, G.E.; Saraswati, S.; Littleton, J.T.; Chouinard, S.W. Development of a Drosophila seizure model for in vivo high-throughput drug screening. *The European journal of neuroscience* **2006**, *24*, 2211-2222, doi:10.1111/j.1460-9568.2006.05075.x.

49. Stewart, R.A.; Li, D.M.; Huang, H.; Xu, T. A genetic screen for modifiers of the lats tumor suppressor gene identifies C-terminal Src kinase as a regulator of cell proliferation in Drosophila. *Oncogene* **2003**, *22*, 6436-6444, doi:10.1038/sj.onc.1206820.

50. Simon, M.A.; Dodson, G.S.; Rubin, G.M. An SH3-SH2-SH3 protein is required for p21Ras1 activation and binds to sevenless and Sos proteins in vitro. *Cell* **1993**, *73*, 169-177.

51. Baker, N.E. Cell proliferation, survival, and death in the Drosophila eye. *Seminars in cell & developmental biology* **2001**, *12*, 499-507, doi:10.1006/scdb.2001.0274.

52. Freeman, M. Reiterative use of the EGF receptor triggers differentiation of all cell types in the Drosophila eye. *Cell* **1996**, *87*, 651-660.

53. Wernet, M.F.; Labhart, T.; Baumann, F.; Mazzoni, E.O.; Pichaud, F.; Desplan, C. Homothorax switches function of Drosophila photoreceptors from color to polarized light sensors. *Cell* **2003**, *115*, 267-279, doi:10.1016/s0092-8674(03)00848-1.

54. Gonzalez, C. Drosophila melanogaster: a model and a tool to investigate malignancy and identify new therapeutics. *Nature reviews. Cancer* **2013**, *13*, 172-183, doi:10.1038/nrc3461.

55. Fogerty, F.J.; Juang, J.L.; Petersen, J.; Clark, M.J.; Hoffmann, F.M.; Mosher, D.F. Dominant effects of the bcr-abl oncogene on Drosophila morphogenesis. *Oncogene* **1999**, *18*, 219-232, doi:10.1038/sj.onc.1202239.

56. Bernardoni, R.; Giordani, G.; Signorino, E.; Monticelli, S.; Messa, F.; Pradotto, M.; Rosso, V.; Bracco, E.; Giangrande, A.; Perini, G., et al. A new BCR-ABL1 Drosophila model as a powerful tool to elucidate pathogenesis and progression of chronic myeloid leukemia. *Haematologica* **2018**, 10.3324/haematol.2018.198267, doi:10.3324/haematol.2018.198267.

57. Basler, K.; Yen, D.; Tomlinson, A.; Hafen, E. Reprogramming cell fate in the developing Drosophila retina: transformation of R7 cells by ectopic expression of rough. *Genes & development* **1990**, *4*, 728-739.

58. Bourbon, H.M.; Gonzy-Treboul, G.; Peronnet, F.; Alin, M.F.; Ardourel, C.; Benassayag, C.; Cribbs, D.; Deutsch, J.; Ferrer, P.; Haenlin, M., et al. A P-insertion screen identifying novel X-linked essential genes in Drosophila. *Mechanisms of development* **2002**, *110*, 71-83.

59. Henriksen, M.A.; Betz, A.; Fuccillo, M.V.; Darnell, J.E., Jr. Negative regulation of STAT92E by an N-terminally truncated STAT protein derived from an alternative promoter site. *Genes & development* **2002**, *16*, 2379-2389, doi:10.1101/gad.1020702.

60. McGuire, S.E.; Mao, Z.; Davis, R.L. Spatiotemporal gene expression targeting with the TARGET and gene-switch systems in Drosophila. *Science's STKE : signal transduction knowledge environment* **2004**, *2004*, pl6, doi:10.1126/stke.2202004pl6.

61. McGuire, S.E.; Roman, G.; Davis, R.L. Gene expression systems in Drosophila: a synthesis of time and space. *Trends in genetics : TIG* **2004**, *20*, 384-391, doi:10.1016/j.tig.2004.06.012.

62. McGuire, S.E.; Le, P.T.; Osborn, A.J.; Matsumoto, K.; Davis, R.L. Spatiotemporal rescue of memory dysfunction in Drosophila. *Science* **2003**, *302*, 1765-1768, doi:10.1126/science.1089035.

63. Giordani, G.; Barraco, M.; Giangrande, A.; Martinelli, G.; Guadagnuolo, V.; Simonetti, G.; Perini, G.; Bernardoni, R. The human Smoothened inhibitor PF-04449913 induces exit from

quiescence and loss of multipotent Drosophila hematopoietic progenitor cells. *Oncotarget* **2016**, *7*, 55313-55327, doi:10.18632/oncotarget.10879.

64. Robinow, S.; White, K. The locus elav of Drosophila melanogaster is expressed in neurons at all developmental stages. *Developmental biology* **1988**, *126*, 294-303.

65. Gertler, F.B.; Hill, K.K.; Clark, M.J.; Hoffmann, F.M. Dosage-sensitive modifiers of Drosophila abl tyrosine kinase function: prospero, a regulator of axonal outgrowth, and disabled, a novel tyrosine kinase substrate. *Genes & development* **1993**, *7*, 441-453.

66. Hill, K.K.; Bedian, V.; Juang, J.L.; Hoffmann, F.M. Genetic interactions between the Drosophila Abelson (Abl) tyrosine kinase and failed axon connections (fax), a novel protein in axon bundles. *Genetics* **1995**, *141*, 595-606.

67. Gertler, F.B.; Bennett, R.L.; Clark, M.J.; Hoffmann, F.M. Drosophila abl tyrosine kinase in embryonic CNS axons: a role in axonogenesis is revealed through dosage-sensitive interactions with disabled. *Cell* **1989**, *58*, 103-113.

68. Gertler, F.B.; Doctor, J.S.; Hoffmann, F.M. Genetic suppression of mutations in the Drosophila abl proto-oncogene homolog. *Science* **1990**, *248*, 857-860.

69. Krause, M.; Bear, J.E.; Loureiro, J.J.; Gertler, F.B. The Ena/VASP enigma. *Journal of cell science* **2002**, *115*, 4721-4726.

70. Grevengoed, E.E.; Fox, D.T.; Gates, J.; Peifer, M. Balancing different types of actin polymerization at distinct sites: roles for Abelson kinase and Enabled. *The Journal of cell biology* **2003**, *163*, 1267-1279, doi:10.1083/jcb.200307026.

71. Grevengoed, E.E.; Loureiro, J.J.; Jesse, T.L.; Peifer, M. Abelson kinase regulates epithelial morphogenesis in Drosophila. *The Journal of cell biology* **2001**, *155*, 1185-1198, doi:10.1083/jcb.200105102.

72. Comer, A.R.; Ahern-Djamali, S.M.; Juang, J.L.; Jackson, P.D.; Hoffmann, F.M. Phosphorylation of Enabled by the Drosophila Abelson tyrosine kinase regulates the in vivo function and protein-protein interactions of Enabled. *Molecular and cellular biology* **1998**, *18*, 152-160.

73. Gertler, F.B.; Comer, A.R.; Juang, J.L.; Ahern, S.M.; Clark, M.J.; Liebl, E.C.; Hoffmann, F.M. enabled, a dosage-sensitive suppressor of mutations in the Drosophila Abl tyrosine kinase, encodes an Abl substrate with SH3 domain-binding properties. *Genes & development* **1995**, *9*, 521-533.

74. Nieborowska-Skorska, M.; Wasik, M.A.; Slupianek, A.; Salomoni, P.; Kitamura, T.; Calabretta, B.; Skorski, T. Signal transducer and activator of transcription (STAT)5 activation by BCR/ABL is dependent on intact Src homology (SH)3 and SH2 domains of BCR/ABL and is required for leukemogenesis. *The Journal of experimental medicine* **1999**, *189*, 1229-1242.

75. de Groot, R.P.; Raaijmakers, J.A.; Lammers, J.W.; Jove, R.; Koenderman, L. STAT5 activation by BCR-Abl contributes to transformation of K562 leukemia cells. *Blood* **1999**, *94*, 1108-1112.

76. Bina, S.; Wright, V.M.; Fisher, K.H.; Milo, M.; Zeidler, M.P. Transcriptional targets of Drosophila JAK/STAT pathway signalling as effectors of haematopoietic tumour formation. *EMBO reports* **2010**, *11*, 201-207, doi:10.1038/embor.2010.1.

77. Zeidler, M.P.; Bach, E.A.; Perrimon, N. The roles of the Drosophila JAK/STAT pathway. *Oncogene* **2000**, *19*, 2598-2606, doi:10.1038/sj.onc.1203482.

78. Le, N.; Simon, M.A. Disabled is a putative adaptor protein that functions during signaling by the sevenless receptor tyrosine kinase. *Molecular and cellular biology* **1998**, *18*, 4844-4854.

79. Song, J.K.; Kannan, R.; Merdes, G.; Singh, J.; Mlodzik, M.; Giniger, E. Disabled is a bona fide component of the Abl signaling network. *Development* **2010**, *137*, 3719-3727, doi:10.1242/dev.050948.

80. McAvoy, S.; Zhu, Y.; Perez, D.S.; James, C.D.; Smith, D.I. Disabled-1 is a large common fragile site gene, inactivated in multiple cancers. *Genes, chromosomes & cancer* **2008**, *47*, 165-174, doi:10.1002/gcc.20519.

81. Finkielstein, C.V.; Capelluto, D.G. Disabled-2: A modular scaffold protein with multifaceted functions in signaling. *BioEssays : news and reviews in molecular, cellular and developmental biology* **2016**, *38 Suppl 1*, S45-55, doi:10.1002/bies.201670907.

82. Zhang, Z.; Chen, Y.; Tang, J.; Xie, X. Frequent loss expression of dab2 and promotor hypermethylation in human cancers: a meta-analysis and systematic review. *Pakistan journal of medical sciences* **2014**, *30*, 432-437.

83. Holz, A.; Bossinger, B.; Strasser, T.; Janning, W.; Klapper, R. The two origins of hemocytes in Drosophila. *Development* **2003**, *130*, 4955-4962, doi:10.1242/dev.00702.

84. Evans, C.J.; Hartenstein, V.; Banerjee, U. Thicker than blood: conserved mechanisms in Drosophila and vertebrate hematopoiesis. *Developmental cell* **2003**, *5*, 673-690.

85. Lanot, R.; Zachary, D.; Holder, F.; Meister, M. Postembryonic hematopoiesis in Drosophila. *Developmental biology* **2001**, *230*, 243-257, doi:10.1006/dbio.2000.0123.

86. Jung, S.H.; Evans, C.J.; Uemura, C.; Banerjee, U. The Drosophila lymph gland as a developmental model of hematopoiesis. *Development* **2005**, *132*, 2521-2533, doi:10.1242/dev.01837.

87. Krzemien, J.; Dubois, L.; Makki, R.; Meister, M.; Vincent, A.; Crozatier, M. Control of blood cell homeostasis in Drosophila larvae by the posterior signalling centre. *Nature* **2007**, *446*, 325-328, doi:10.1038/nature05650.

88. Lebestky, T.; Jung, S.H.; Banerjee, U. A Serrate-expressing signaling center controls Drosophila hematopoiesis. *Genes & development* **2003**, *17*, 348-353, doi:10.1101/gad.1052803.

89. Luo, H.; Hanratty, W.P.; Dearolf, C.R. An amino acid substitution in the Drosophila hopTum-l Jak kinase causes leukemia-like hematopoietic defects. *The EMBO journal* **1995**, *14*, 1412-1420.

90. Minakhina, S.; Steward, R. Melanotic mutants in Drosophila: pathways and phenotypes. *Genetics* **2006**, *174*, 253-263, doi:10.1534/genetics.106.061978.

91. Irving, P.; Ubeda, J.M.; Doucet, D.; Troxler, L.; Lagueux, M.; Zachary, D.; Hoffmann, J.A.; Hetru, C.; Meister, M. New insights into Drosophila larval haemocyte functions through genome-wide analysis. *Cellular microbiology* **2005**, *7*, 335-350, doi:10.1111/j.1462-5822.2004.00462.x.

92. Ellis, M.C.; O'Neill, E.M.; Rubin, G.M. Expression of Drosophila glass protein and evidence for negative regulation of its activity in non-neuronal cells by another DNA-binding protein. *Development* **1993**, *119*, 855-865.

93. Bennett, R.L.; Hoffmann, F.M. Increased levels of the Drosophila Abelson tyrosine kinase in nerves and muscles: subcellular localization and mutant phenotypes imply a role in cell-cell interactions. *Development* **1992**, *116*, 953-966.

94. Xiong, W.; Morillo, S.A.; Rebay, I. The Abelson tyrosine kinase regulates Notch endocytosis and signaling to maintain neuronal cell fate in Drosophila photoreceptors. *Development* **2013**, *140*, 176-184, doi:10.1242/dev.088799.

95. Barzik, M.; Kotova, T.I.; Higgs, H.N.; Hazelwood, L.; Hanein, D.; Gertler, F.B.; Schafer, D.A. Ena/VASP proteins enhance actin polymerization in the presence of barbed end capping proteins. *The Journal of biological chemistry* **2005**, *280*, 28653-28662, doi:10.1074/jbc.M503957200.

96. Bear, J.E.; Svitkina, T.M.; Krause, M.; Schafer, D.A.; Loureiro, J.J.; Strasser, G.A.; Maly, I.V.; Chaga, O.Y.; Cooper, J.A.; Borisy, G.G., et al. Antagonism between Ena/VASP proteins and actin filament capping regulates fibroblast motility. *Cell* **2002**, *109*, 509-521.

97. Olivier, J.P.; Raabe, T.; Henkemeyer, M.; Dickson, B.; Mbamalu, G.; Margolis, B.; Schlessinger, J.; Hafen, E.; Pawson, T. A Drosophila SH2-SH3 adaptor protein implicated in coupling the sevenless tyrosine kinase to an activator of Ras guanine nucleotide exchange, Sos. *Cell* **1993**, *73*, 179-191.

98. Villavicencio, E.H.; Walterhouse, D.O.; Iannaccone, P.M. The sonic hedgehog-patched-gli pathway in human development and disease. *American journal of human genetics* **2000**, *67*, 1047-1054, doi:10.1016/S0002-9297(07)62934-6.

99. Queiroz, K.C.; Ruela-de-Sousa, R.R.; Fuhler, G.M.; Aberson, H.L.; Ferreira, C.V.; Peppelenbosch, M.P.; Spek, C.A. Hedgehog signaling maintains chemoresistance in myeloid leukemic cells. *Oncogene* **2010**, *29*, 6314-6322, doi:10.1038/onc.2010.375.

100. Zhao, C.; Chen, A.; Jamieson, C.H.; Fereshteh, M.; Abrahamsson, A.; Blum, J.; Kwon, H.Y.; Kim, J.; Chute, J.P.; Rizzieri, D., et al. Hedgehog signalling is essential for maintenance of cancer stem cells in myeloid leukaemia. *Nature* **2009**, *458*, 776-779, doi:10.1038/nature07737.

101. Abd Elrhman, H.E.; Ebian, H.F. Patched homolog 1 (PTCHI) gene mutations can predict the outcome of chronic myeloid leukemia patients? *American journal of blood research* **2019**, *9*, 15-24.

102. Alonso-Dominguez, J.M.; Grinfeld, J.; Alikian, M.; Marin, D.; Reid, A.; Daghistani, M.; Hedgley, C.; O'Brien, S.; Clark, R.E.; Apperley, J., et al. PTCH1 expression at diagnosis predicts imatinib failure in chronic myeloid leukaemia patients in chronic phase. *American journal of hematology* **2015**, *90*, 20-26, doi:10.1002/ajh.23857.

103. Cea, M.; Cagnetta, A.; Cirmena, G.; Garuti, A.; Rocco, I.; Palermo, C.; Pierri, I.; Reverberi, D.; Nencioni, A.; Ballestrero, A., et al. Tracking molecular relapse of chronic myeloid leukemia by measuring Hedgehog signaling status. *Leukemia & lymphoma* **2013**, *54*, 342-352, doi:10.3109/10428194.2012.708752.

104. Long, B.; Zhu, H.; Zhu, C.; Liu, T.; Meng, W. Activation of the Hedgehog pathway in chronic myelogeneous leukemia patients. *Journal of experimental & clinical cancer research : CR* **2011**, *30*, 8, doi:10.1186/1756-9966-30-8.

105. Shyamala, B.V.; Bhat, K.M. A positive role for patched-smoothened signaling in promoting cell proliferation during normal head development in Drosophila. *Development* **2002**, *129*, 1839-1847.

106. Su, E.; Han, X.; Jiang, G. The transforming growth factor beta 1/SMAD signaling pathway involved in human chronic myeloid leukemia. *Tumori* **2010**, *96*, 659-666.

107. Liu, N.; Zang, S.; Liu, Y.; Wang, Y.; Li, W.; Liu, Q.; Ji, M.; Ma, D.; Ji, C. FZD7 regulates BMSCs-mediated protection of CML cells. *Oncotarget* **2016**, *7*, 6175-6187, doi:10.18632/oncotarget.6742.

108. Luo, J.; Yu, F.X. GPCR-Hippo Signaling in Cancer. *Cells* **2019**, *8*, doi:10.3390/cells8050426.

109. Zhang, B.; Groffen, J.; Heisterkamp, N. Increased resistance to a farnesyltransferase inhibitor by N-cadherin expression in Bcr/Abl-P190 lymphoblastic leukemia cells. *Leukemia* **2007**, *21*, 1189-1197, doi:10.1038/sj.leu.2404667.

110. Mu, H.J.; Xie, R.; Shen, Y.F.; Jiang, Y.Q.; Zeng, Y.J. Cadherin-13 in primary and blast crisis chronic myeloid leukaemia: declining expression and negative correlation with the BCR/ABL fusion gene. *British journal of biomedical science* **2009**, *66*, 20-24, doi:10.1080/09674845.2009.11730239.

111. Yuan, W.; Song, C. The Emerging Role of Rab5 in Membrane Receptor Trafficking and Signaling Pathways. *Biochemistry research international* **2020**, *2020*, 4186308, doi:10.1155/2020/4186308.

112. Trino, S.; De Luca, L.; Simeon, V.; Laurenzana, I.; Morano, A.; Caivano, A.; La Rocca, F.; Pietrantuono, G.; Bianchino, G.; Grieco, V., et al. Inverse regulation of bridging integrator 1 and BCR-ABL1 in chronic myeloid leukemia. *Tumour biology : the journal of the International Society for Oncodevelopmental Biology and Medicine* **2016**, *37*, 217-225, doi:10.1007/s13277-015-3772-9.